SLAC - PUB - 4673
SCIPP 88/27
August 1988
(T/E)

MEASURING CP VIOLATION IN THE $B^0\overline{B}^0$ SYSTEM WITH ASYMMETRIC ENERGY e^+e^- BEAMS*

R. ALEKSAN,† J. BARTELT

Stanford Linear Accelerator Center
Stanford University, Stanford, California 94309

P. R. BURCHAT, A. SEIDEN

Santa Cruz Institute for Particle Physics
University of California, Santa Cruz, CA 95064

Submitted to Physical Review D

---

* Work supported by Department of Energy contracts DE-AC03-76SF00515 and DE-AM03-76SF00010

† on leave of absence from C.E.N. Saclay DPHPE/SEPH, 91191 GIF/Yvette, France

ABSTRACT

We have studied in some detail the possibility of observing CP violation in the B meson system using asymmetric energy e^+e^- beams colliding with a center-of-mass energy corresponding to the $\Upsilon(4S)$ mass. If a CP eigenstate is detected in conjunction with an identified B^0 or $\overline{B}^0$, the distribution of the flight path between decays contains a term which provides a measurement of CP violation, as discussed in this paper. The moving B mesons in the laboratory make this flight path measurement possible. The use of the $\Upsilon(4S)$ provides the largest $B\overline{B}$ cross section in e^+e^- production, other than from the Z^0, and allows excellent background rejection because the B is monoenergetic in the center-of-mass frame. Since there are no extra fragmentation products accompanying the $B\overline{B}$ in the event, very simple tagging strategies can be used to separate B^0 from $\overline{B}^0$ decays, providing a tagging efficiency close to 50%. The CP eigenstates studied in this paper are $J/\psi K^0_S$, $J/\psi K^{*0}$ and $\psi' K^0_S$. Given an adequate detector, the integrated luminosity needed to observe CP violation in the Standard Model is expected to be about 2×10^{40} cm^{-2} or 10^7 produced $B^0\overline{B}^0$ pairs.

1. Introduction

Two important measurements have recently spurred interest in the potential of B meson physics to provide tests of the Standard Model. The first is the measurement of the long lifetime of the B mesons[1] ($\tau_B \simeq 1.2$ ps). This long lifetime, together with the recent development of precise vertex detection techniques, make the observation of detached B vertices possible. Secondly, a high degree of mixing between B^0 and $\overline{B}^0$ has been reported.[2] This introduces a promising possibility for measuring CP violation in the B system. This would be the first detection of CP violation outside the K^0 system.

We outline in this paper a method for measuring this possible CP violation which takes advantage of the long lifetime of the B meson. We discuss the advantages of an asymmetric energy e^+e^- collider, the physics behind CP violation in the B system, and our analysis methods. We conclude that the integrated luminosity needed to observe CP violation in the Standard Model at the $\Upsilon(4S)$ is expected to be about 2×10^{40} cm^{-2} or 10^7 produced $B^0\overline{B}^0$ pairs.

1.1 WHY AN ASYMMETRIC ENERGY COLLIDER?

Most measurements of the b quark sector (with the exception of the Υ discovery itself) come from e^+e^- colliders operating in two energy regions which offer complementary advantages and disadvantages: (1) a center-of-mass energy equal to the $\Upsilon(4S)$ mass where the cross section is high and exclusive $B\overline{B}$ final states are produced with the B mesons essentially at rest, or (2) a center-of-mass energy in the continuum where the cross section is lower and inclusive final states are produced, but the B mesons are moving in the laboratory frame, enabling lifetime measurements.

In addition to the higher rate for producing $B\overline{B}$ exclusive states on the $\Upsilon(4S)$ resonance, there are several other advantages. Since only two B mesons are produced, one can use the constraint that each B meson energy equal the beam energy to reduce the combinatorial background when reconstructing final states.

Another benefit of exclusive $B\overline{B}$ states is that having tagged one of the B's as a B_u or B_d, one is guaranteed that the second B is of the same type. Furthermore, there is a great advantage in having produced two spin-0 particles in a p-wave state. Because of Bose statistics, a $B^0\overline{B}^0$ pair will remain in a coherent $B^0\overline{B}^0$ or B_1B_2 state as long as neither B has decayed. This remark is extremely important for measuring mixing or CP violation. In fact, one of the most promising ways to observe CP violation in the b sector is to use the B decays to CP eigenstates f_{CP} where CP violation comes from the interference of the amplitudes $A(B^0 \to f_{CP})$ and $A(B^0 \to \overline{B}^0 \to f_{CP})$. In order to detect this CP violation, one must know the nature of the particle (B^0 or $\overline{B}^0$) at a given time. On the Υ(4S), tagging one B as a B^0 or a $\overline{B}^0$ identifies the other with certainty.

However, one must also measure the time order of the decays to be sensitive to CP violation. Since the B mesons are produced almost at rest – the B momentum is about 330 MeV – a measurement of the B lifetimes and consequently any time dependence is impossible with the present status of vertex detection. The average decay length of the B's is about 20 μm.

The conclusion is that despite the advantages that one gains with a center-of-mass energy equal to the mass of the $\Upsilon(4S)$, it is currently not practical to study any time dependence of the B decays and therefore it is not possible to measure CP violation using the $B^0\overline{B}^0$ mixing scenario outlined above.

One way to produce B mesons moving in the laboratory frame is to operate at a center-of-mass energy in the continuum above the Υ resonances. At a center-of-mass energy of 15 GeV, the average decay length of the B mesons is about 300 μm, a decay length which can be measured with present technologies. Unfortunately, there are also disadvantages in this energy region.

First, the cross section is lower by a factor of eight at a center-of-mass energy of 15 GeV compared with the Υ(4S). Since the B mesons are no longer produced with the beam energy, one must fully reconstruct a B in order to determine its momentum to study time dependence. Furthermore, mixing and CP violation

studies are more complicated for the following reason. Since the quantum coherence of the initial state is lost, each B meson state can evolve independently of the other B state. This means that tagging the second B does not guarantee that one has determined the real nature of the first one at the time of production. As an example, a high energy positron might tag a B^+, a B^0, or a $\overline{B}^0$ which has mixed to a B^0. The effect of the $B_s^0\overline{B}_s^0$ and $B_d^0\overline{B}_d^0$ mixing is to produce an apparent dilution of the CP violation asymmetry. This dilution requires a factor of two more events to make a measurement of the same statistical significance. Together with the lower cross section, one suffers so greatly in terms of rate that the advantage of having moving B's in the laboratory frame is lost.

A solution for overcoming the disadvantages of the two previous schemes while retaining their positive aspects is to produce the Υ resonances moving in the laboratory frame. This can be achieved by colliding two beams of unequal energy.[3] This results in two B's boosted in the same direction along the beam axis. The average distance between the two B decays is approximately $c\beta\gamma\tau$ where β and γ are the boost parameters of the center of mass and τ is the average B lifetime. This method allows both the production of exclusive B meson states with a relatively large cross-section and the measurement of the lifetimes that enable the detection of a violation of CP symmetry.

In the next section, we review the formalism for CP violation and the choices of CP eigenstates. In section 3, we outline the physics processes, detector parameters and collider configuration which were simulated through Monte Carlo techniques for this study. The method for finding vertices in the $B\overline{B}$ events is described in section 4 and, in section 5, we outline the analysis procedure for measuring CP violation in the B sector. In the last section, we conclude with a description of a possible detector for studying B physics at an asymmetric collider, and a summary of the number of reconstructed, tagged events we expect for a CP violation study with a data sample of 10^7 $B^0\overline{B}^0$ pairs.

2. CP Violation Using CP Eigenstates at the $\Upsilon(4S)$

2.1 FORMALISM

The $\Upsilon(4S)$ decays into $B^0\overline{B}^0$ in a p-wave state which imposes special correlations on the final state.[4] The unique initial state implies that if the first neutral B decays into a final state f_1 at time t_1, this projects the remaining neutral B onto the orthogonal state which cannot decay into f_1. This state then propagates in time and we observe its decay at time t_2 into final state f_2. We can think of the first decay as preparing the second B in a special state at t_1, whose propagation then depends only on the time difference $t_2 - t_1$.

The final states f_1 or f_2 that are observed can either be unique to B^0 or $\overline{B}^0$ only (for example, the primary decay into a lepton of a given charge) or can receive contributions from both types of B. In the case of a CP eigenstate for f_1 or f_2, the contributions from each B are essentially equal in magnitude. A decay unique to B^0 or $\overline{B}^0$ is said to tag the B flavor. We can measure mixing in the B system if both f_1 and f_2 are tagging decays. CP violation can be measured, in the presence of mixing, if one decay is a tagging decay and the other is a CP eigenstate. Decay into two eigenstates of the same CP would also measure CP violation,[5] but the rates in this case are probably too small to be useful.

The decay to a tagging state plus a CP eigenstate provides four configurations which have to be separately analyzed as a function of $t_2 - t_1$ in order to measure CP violation. For the possible final states which provide a B^0 tag (f_B), a $\overline{B}^0$ tag ($f_{\overline{B}}$) or a CP eigenstate ($f_{\rm CP}$), the choices of decays and associated times are:

(1) $f_B(t_1) f_{\rm CP}(t_2)$,

(2) $f_{\rm CP}(t_1) f_B(t_2)$,

(3) $f_{\overline{B}}(t_1) f_{\rm CP}(t_2)$,

(4) $f_{\rm CP}(t_1) f_{\overline{B}}(t_2)$.

If CP violation exists in the B system, (1) and (4) have a distribution in $t_2 - t_1$ which is different from that of (2) and (3). Summing over (1) and (2) or (3) and (4), as would be done if no vertex information were available, removes the CP violating effect. A measure of CP violation is given by the asymmetry in rates

$$A = \frac{(2) + (3) - (1) - (4)}{(1) + (4) + (2) + (3)}$$

where each term is integrated over the same positive time interval of $t_2 - t_1$. A change of sign of the CP of the state is equivalent to exchanging B and $\overline{B}$ and therefore changes the sign of A.

We sketch below, to a very good approximation, the calculation of the rates for (1) and (2), as expected for a CP even state. The mass eigenstates of definite lifetime for the B system are

$$B_1^0 = \frac{e^{i\phi_1} B^0 + e^{-i\phi_1} \overline{B}^0}{\sqrt{2}}, \quad B_2^0 = \frac{e^{i\phi_1} B^0 - e^{-i\phi_1} \overline{B}^0}{\sqrt{2}} ,$$

giving

$$B^0 = \left(\frac{B_1^0 + B_2^0}{\sqrt{2}} \right) e^{-i\phi_1}, \quad \overline{B}^0 = \frac{(B_1^0 - B_2^0)}{\sqrt{2}} e^{i\phi_1} .$$

We define

$$m \equiv \frac{m_1 + m_2}{2}, \ \Gamma \equiv \frac{\Gamma_1 + \Gamma_2}{2}, \ \Delta m \equiv m_2 - m_1 \ \text{ and } \Delta\Gamma \equiv \Gamma_2 - \Gamma_1.$$

Under reasonable assumptions in the Standard Model,[6] it is expected that $\Delta\Gamma \ll \Gamma$ and $\Delta\Gamma \ll \Delta m$. Under these assumptions, the time evolution of B_1^0 and B_2^0 is given by

$$B_1^0(t) = B_1^0 e^{-(\Gamma t/2 + imt)} e^{i\Delta m t/2}$$
$$B_2^0(t) = B_2^0 e^{-(\Gamma t/2 + imt)} e^{-i\Delta m t/2} .$$

We take for the decay amplitudes

$$\langle f_B | H_w | B^0 \rangle = \mathcal{B}, \qquad \langle f_B | H_w | \overline{B}^0 \rangle = 0,$$
$$\langle f_{\rm CP} | H_w | B^0 \rangle = \mathcal{A} e^{i\phi_2}, \qquad \langle f_{\rm CP} | H_w | \overline{B}^0 \rangle = \mathcal{A}' e^{-i\phi_2}.$$

where H_w is the weak decay Hamiltonian, and ϕ_2 is the phase from the Kobayashi-Maskawa (K–M) matrix. In the following we shall let $\mathcal{A} = \mathcal{A}'$, which is a safe approximation.

The phases in the individual formulae shown above depend on the phase convention for the K–M matrix. However, the final result below contains one phase which is a measurable invariant of the matrix and is independent of conventions.[7]

For process (1), the state projected at t_1 is $\overline{B}^0$. With $t \equiv t_2 - t_1$, the rate to later detect $f_{\rm CP}$ is proportional to $|\langle f_{\rm CP}| H_w |\overline{B}^0(t)\rangle|^2$. For process (2), the state projected at t_1 is $(B^0 e^{-i\phi_2} - \overline{B}^0 e^{i\phi_2})/\sqrt{2}$ and therefore the rate to subsequently detect f_B is proportional to $|\langle f_B| H_w |(B^0(t)e^{-i\phi_2} - \overline{B}^0(t)e^{i\phi_2})/\sqrt{2}\rangle|^2$. Inserting the time evolution of $B^0(t)$ and $\overline{B}^0(t)$, through their dependence on $B_1^0(t)$ and $B_2^0(t)$, and the decay amplitudes, we get:

the rate for $f_B(t_1) f_{\rm CP}(t_2)$ is proportional to $|\mathcal{A}|^2 |\mathcal{B}|^2 [1 - \sin(2\phi)\sin(\Delta m t)]\, e^{-\Gamma t}$,
the rate for $f_{\rm CP}(t_1) f_B(t_2)$ is proportional to $|\mathcal{A}|^2 |\mathcal{B}|^2 [1 + \sin(2\phi)\sin(\Delta m t)]\, e^{-\Gamma t}$,

where $\phi = \phi_1 + \phi_2$. The CP violating asymmetry depends on the phase ϕ, which in principle can be calculated from the K–M matrix, and the presence of mixing which depends on the magnitude of $\Delta m/\Gamma$.

Note that if the Standard Model is not a complete description of weak interactions, observing CP violation in only one channel (*e.g.*, $J/\psi K_S^0$) does not allow us to determine whether the CP violation originates in the mixing ($\Delta B = 2$) or in the decay ($\Delta B = 1$). It is therefore necessary to observe CP violation with sufficient accuracy in another decay mode in order to distinguish between different models: for example, to disprove the superweak model.[8]

2.2 MEASUREMENT FOR A MOVING $\Upsilon(4S)$ SYSTEM

For a moving $\Upsilon(4S)$ system, where the momentum of the B in the $\Upsilon(4S)$ rest frame can be ignored (this approximation will be discussed in Sec. 3.3), the distribution in t translates directly into the distribution between the B decay vertex positions along the flight direction of the B systems. For $\beta\gamma = 1$ for each B this difference in position is $\Delta z \simeq ct$, and therefore has a mean value of $c\tau \simeq 300$ μm. The point of creation of the $\Upsilon(4S)$, which is not measurable, is fortunately not needed for the analysis.

The CP dependent asymmetry, defined earlier, is given by

$$A = \left[\frac{\int_{t_0}^{\infty} \sin(\Delta m t) e^{-\Gamma t} dt}{\int_{t_0}^{\infty} e^{-\Gamma t} dt}\right] \sin 2\phi$$

$$= \frac{\left[\sin(\Delta m \tau_0/\Gamma) + (\Delta m/\Gamma)\cos(\Delta m \tau_0/\Gamma)\right]}{1 + (\Delta m/\Gamma)^2} \sin 2\phi \ ,$$

where $\tau_0 = t_0\Gamma$. If all events are used, $\tau_0 = 0$, and

$$A = \frac{(\Delta m/\Gamma)\sin 2\phi}{1 + (\Delta m/\Gamma)^2} \ .$$

If N detected events are available in total, then the error on the asymmetry is given by $\delta A = \sqrt{(1 - A^2)/N}$. Since A is expected to be $\sim$ 0.1 to 0.3 in the Standard Model,[9] a goal of at least 1000 events should be set, as this would then give $\delta A \sim 0.03$.

A cut requiring a non-zero τ_0 would increase A at the cost of reducing N. For $\Delta m/\Gamma \simeq 0.75$, a cut requiring $\tau_0 \gtrsim 0.6$ increases the significance in terms of the number of standard deviations, $\delta A/A$, by about 20%. Finally, we point out that the measurement allows several important internal checks since the asymmetry changes sign if we exchange B^0 and $\overline{B}^0$, the CP of the final state, or the time ordering of the two B decays.

Detectable CP eigenstates are the CP odd decays $J/\psi K_S^0$ and $\psi' K_S^0$, and the CP even decays $J/\psi K_S^0 \pi^0$ (from K^{*0} decay) and $D\overline{D}$. With a detector which includes a tracking calorimeter, it might even be possible to measure the CP even decay $J/\psi K_L^0$ by reconstructing the flight direction of the K_L^0 from its interaction point in the calorimeter.

The analysis discussed above for the exclusive $B^0\overline{B}^0$ final state from $\Upsilon(4S)$ is very different from the high energy inclusive limit in e^+e^- production where one must measure the unambiguous presence of a b or $\bar{b}$ in one jet in conjunction with the time evolution of the decay to a CP eigenstate in the other jet. In that case, the relevant time is with respect to the primary production vertex. The region in energy somewhat above the $\Upsilon(4S)$ contains a strongly energy dependent mixture of several exclusive final states. An optimum and appropriate analysis for this region therefore requires careful consideration as neither our exclusive analysis nor the inclusive analysis is correct.

3. The $B\overline{B}$ Monte Carlo

3.1 THE FOUR-VECTOR GENERATOR

In order to study different topics in $B\overline{B}$ physics, we have written a four-vector generator that is interfaced to the GEANT[10] detector simulation package. This program generates B^+B^- or $B^0\overline{B}^0$ final states for a moving center of mass. In the center-of-mass frame, the B's are generated with a $\sin^2\theta$ distribution with respect to the beam direction.

Branching ratios

In the simulation, the B mesons decay either semileptonically or purely hadronically. The semileptonic branching ratios are set to 12% each for e and μ and 2% for τ. These decays come from the coupling of the W to the b quark

(Fig. 1) and therefore exhibit the standard momentum distribution for V–A coupling. The remaining spectator quark is then combined with the c quark to form a D or D^* meson with probabilities of 30% and 70%, respectively.

The purely hadronic decays are more difficult to simulate since we know little at present about the exclusive hadronic decays of the B mesons. We therefore use a simple model for these decays. The B meson is treated as decaying to a four-quark final state with the following branching fractions:

$$B(B_q \to \bar{c}q\bar{d}u) = 62\%\,,\ B(B_q \to \bar{c}q\bar{s}c) = 13\%\,.$$

Having selected a four quark final state, we select a total multiplicity for primary produced mesons according to a gaussian distribution with mean 4.7 and variance 3.2 . The decay multiplicity is bounded between two and ten. If the multiplicity is greater than two, we add as many $q\bar{q}$ pairs to the four quark system as needed to meet the final state requirement. The quarks are then assigned to $q_1\bar{q}_2$ pairs in a random way. For each $q_1\bar{q}_2$ pair, we form a spin-0 or spin-1 meson. The ratio of pseudoscalar to vector mesons is chosen to be 1:2. The hadronic decay products are distributed according to a phase space angular distribution in the B rest frame.

We feel that for this study, great accuracy in the hadronic decays of the B is not necessary. The semileptonic B decays and the charmed meson decays are more important since these are the decays used for tagging B flavor. Fortunately, these are relatively well understood and therefore are accurately simulated by the generator.

Once the B decay is simulated, all unstable mesons decay. We use the branching ratios tabulated by the Particle Data Group[11] for these secondary particles. The D^+, D^-, D^0 and $\overline{D}^0$ mesons are exceptions for which we use the most recently measured branching fractions.[12] 20% of the charged D decays and 10% of the neutral D decays have not been measured. For these decays, we produce

final states with at least two neutral pions. The D_s decays are simulated using the same method as for the B meson. We have checked that the generator is reproducing the measured decay modes[12] reasonably well.

Decay length of longlived mesons

Since the measurement of the distance between the primary B decays is a critical part of the CP violation measurement described in this paper, the generator must simulate the flight distance of all longlived particles such as B and D mesons. Their lifetimes have been set to the following values: $\tau(D^0) = 0.44$ ps, $\tau(D^+) = 1.10$ ps, $\tau(D_s^+) = 0.40$ ps, $\tau(B^+) = 1.10$ ps and $\tau(B^0) = 1.10$ ps.

Mixing

The generator allows for $B_d^0\overline{B}_d^0$ mixing. As mentioned above, at the $\Upsilon(4S)$, both B^0 and $\overline{B}^0$ – or equivalently B_1 and B_2 – are in a coherent state, because of Bose statistics, until one of the B's decays. This is very important experimentally. It means that the relevant starting time for time-dependence studies is the time at which the first B decays and not the time at which both B's were produced. This is very fortunate since the experimentally measurable quantity is the distance between B decays if this distance is large enough. We cannot measure the distance the B's travelled together before the first one decayed since the beam size is much larger in this direction than the B decay length. In the study described below, we assume the beam size is 400 μm in the horizontal transverse dimension, 40 μm in the vertical transverse dimension and 2 cm in z.

As soon as one of the B's decays (at time t_1), it fixes the nature of the second B. The time dependence for the mixing between B^0 and $\overline{B}^0$ can be seen in the probability to observe a B meson decay as a B^0 or $\overline{B}^0$ at time t_2 if it was a B^0 at time t_1:

$$\Pr(B^0(t_1) \to \overline{B}^0(t_2)) \;\propto\; \frac{e^{-\Gamma(t_2-t_1)}\Big[1-\cos(x\Gamma(t_2-t_1))\Big]}{2}$$

and

$$\Pr(B^0(t_1) \to B^0(t_2)) \;\propto\; \frac{e^{-\Gamma(t_2-t_1)}\Big[1+\cos(x\Gamma(t_2-t_1))\Big]}{2}$$

where $x \equiv \frac{\Delta m}{\Gamma}$ represents the amount of mixing and has been measured by the Argus collaboration[2] to be $0.73^{+0.17}_{-0.19}$ for the $B^0_d\overline{B}^0_d$ system. For this analysis it has been set to 0.75 for the $B^0_d\overline{B}^0_d$ system.

3.2 Detector simulation

Because an important part of this analysis is the measurement of the B vertices and their relative location, accurate simulation of the multiple scattering of particles in matter is essential. We use the GEANT detector simulation package since in the framework of GEANT it is very easy to simulate any detector and moreover to modify it by changing the materials that are used, their thicknesses or their dimensions. In addition to the multiple scattering, this package simulates all the other interactions or reactions that degrade the measurements such as bremsstrahlung, nuclear interactions, pair production, Compton scattering and decays of very longlived particles such as kaons or charged pions. The penalty for using this package is the large amount of computing time that is needed to simulate one event. Therefore, we only simulate the vertex detector environment in detail. We feel that accurately simulating a central detector and calorimeter is not necessary for this study. We simulate these detectors by simply smearing the momentum of a charged particle and the energy and angles of a neutral particle according to normal distributions with the following standard deviations:

$$\frac{\sigma_{p_T}}{p_T} \;=\; 0.005\sqrt{1+p_T^2},\quad \frac{\sigma_E}{E} \;=\; \frac{0.02}{\sqrt[4]{E}},\quad \sigma_\theta \;=\; 0.02 \text{ radian.}$$

In the above formulae, p_T and E are measured in units of GeV. The angular resolution for the charged particles is then mainly due to the multiple scattering and the vertex detector resolution.

The important points for obtaining good vertex reconstruction are the amount of material before the first two measurements, the distance between the interaction point and the first measurement, and the vertex detector resolution. We simulate a 1 mm thick beryllium beam pipe at a radius of 10 mm, with two layers of silicon pixel detectors, as shown in Fig. 2. The silicon thickness has been set to 300 μm; the two layers are located at radii of 1.2 cm and 4.2 cm and extend 30 cm in both the forward and backward directions. The pixel resolution is set to 10 μm. It will be clear from the next section that one wants to avoid using a beam pipe with a radius much larger than about 10 mm.

3.3 The Boost

The choice of center-of-mass boost depends upon the desired separation between the two B decays, detector resolutions and detector acceptances. To illustrate this, consider a 0.5 GeV/c particle emitted with a polar angle of 90° in a symmetric machine. With a moving center of mass with $\beta\gamma = 1$ ($E_{e^\pm} = 12.5$ GeV, $E_{e^\mp} = 2.3$ GeV), the polar angle will be 45° and the momentum 0.7 GeV/c in the laboratory frame. These values would be 11° and 2.5/c GeV for $\beta\gamma = 5$. It is obvious from these numbers that one would not use the same vertex detector geometry in both examples. This makes the comparison somewhat more difficult. However let us suppose for the moment that in both cases we are able to use a beam pipe with the same radius and with a negligible thickness relative to the first vertex detector layer. Let us assume pixel devices for the vertex detector, with the cylindrical geometry described in the previous section for the $\beta\gamma = 1$ case, and assume a series of planar detectors perpendicular to the beampipe for the $\beta\gamma = 5$ case. We can estimate the error σ_z on the reconstructed z position of a track. In the first scheme ($\beta\gamma = 1$), we can approximate the error due to multiple scattering with the formula for a cylindrical detector

$$\sigma_z^a \simeq \frac{0.014R\sqrt{X}}{p\sin^{5/2}\theta},$$

and in the second scheme ($\beta\gamma = 5$), with the formula for planar detectors

$$\sigma_z^b \simeq \frac{0.014R\sqrt{X}}{p\sin^2\theta}$$

where R is the beam pipe radius, X the number of radiation lengths seen by the particle, p the particle momentum, and θ the polar angle of the particle in the laboratory frame.

Applying these formulae for our test particle and using $R = 10$ mm and $X = 3 \times 10^{-3}$, we obtain

$$\frac{< z_B - z_{\overline{B}} >^a}{\sigma_z^a} = 12 \quad \text{and} \quad \frac{< z_B - z_{\overline{B}} >^b}{\sigma_z^b} = 19\,.$$

With this simple approximation, we conclude that the larger boost is better. However, this difference tends to diminish if we introduce the beam pipe thickness and vertex detector resolution. In addition, $\beta\gamma$=5 implies a very asymmetric machine ($E_{e^\pm} = 50$ GeV, $E_{e^\mp} = 0.5$ GeV) which is more difficult to build and would lead to more severe synchrotron radiation problems since the vertex detector would be at much smaller angles. We have therefore chosen to study the relatively small boost scenario corresponding to $\beta\gamma = 1$ which would be easier to build and could make use of existing facilities such as PEP or PETRA.

$\beta\gamma = 1$ along the beam direction

With a boosted center of mass, all the particle directions are folded forward. One can estimate this folding by using the approximation of relativistic particles. Since the boost is along the beam direction, the transverse component of the momentum is unchanged and the longitudinal momentum of B meson decay products is given by

$$p_z^{Lab} \simeq p_z^{cm}\gamma + p^{cm}\beta\gamma,$$

$$p^{Lab} \simeq p_z^{cm}\beta\gamma + p^{cm}\gamma.$$

Hence

$$\cos(\theta^{Lab}) \simeq \frac{p_z^{cm}\sqrt{2} + p^{cm}}{p^{cm}\sqrt{2} + p_z^{cm}} = \frac{1 + \sqrt{2}\cos\theta^{cm}}{\sqrt{2} + \cos\theta^{cm}}.$$

Particles emitted at a relatively large angle in the center-of-mass frame ($|\cos\theta| \lesssim 0.7$), will have their angle divided by roughly two. Fig. 3 shows the distribution of polar angle for final state particles in the laboratory frame. The momentum of most of the particles will be increased slightly compared to a symmetric machine, particularly for particles emitted at small forward angles. This is fortunate since these particles will cross more material than the ones emitted at large angles. Fig. 4 shows the pion momentum spectrum.

For mixing or CP violation studies, one needs to relate the measured longitudinal distance between the two B decays Δz to the time difference between decays $t \equiv t_2 - t_1$, where t_1 and t_2 are the lifetimes measured in the respective rest frames of the B mesons. In the approximation that the two B's are produced at rest in the $\Upsilon(4S)$ rest frame, the relationship is simply

$$\Delta z = c\beta\gamma t\,.$$

The exact relationship in terms of the velocity β^{cm}, the Lorentz factor γ^{cm} and the polar angle θ^{cm} of the B in the event center of mass is

$$\Delta z = c\beta\gamma\gamma^{cm}t + c\gamma\beta^{cm}\gamma^{cm}\cos\theta^{cm}(2t_1 + t).$$

Reconstructing the momentum of one of the B's does not allow exact evaluation of t since t_1 is unknown. Fortunately, since β^{cm} is only about 0.07, γ^{cm} is very near 1 (≈ 1.003), and the polar angle distribution of the B meson in the center-of-mass system is peaked at large angles, the average error on t due to the above approximation is only on the order of 8% in proper time units. One can see from Fig. 5 that even in a large mixing scenario ($\frac{\Delta m}{\Gamma} = 5$) this approximation produces negligible smearing of the time distribution.

4. Vertex Reconstruction

In this section we describe the algorithm used to reconstruct primary B and D decay vertices. It is based on the detector model discussed earlier and assumes that the position errors at the vertex location are dominated by the resolution of the vertex detector and the multiple scattering in the beampipe and vertex detector.

The algorithm begins by extrapolating each track back to its distance of closest approach to the z axis which is centered on the beam–beam collision region and points along the direction of motion of the $\Upsilon(4S)$ system. B and D meson vertices are expected to be separated by less than a few hundred microns in the plane perpendicular to this axis and to lie in a few centimeter long region along this axis. In addition, the two primary B decays are expected to be very close to each other in the transverse plane (*i.e.*, to have the same x and y coordinates but different z coordinates) since they have very little transverse momentum and therefore nearly follow the trajectory of the parent $\Upsilon(4S)$ in the laboratory. Note that this is a very important constraint since it allows one to identify a primary B vertex without having to fully reconstruct B or D mesons, by matching its x, y coordinates with those of a kinematically reconstructed B meson.

At the distance of closest approach to the z axis, each track has a calculated position $\vec{x}$, tangent unit vector $\vec{t}$ and transverse position error σ. We use the fact that we know a priori that the vertex lies within a cylinder along the z axis of radius a few millimeters to assign an error matrix to each track's position as follows:

$$M_{ij} = \sigma^2 \delta_{ij} + r^2 t_i t_j \ .$$

We choose the cylinder radius to be 5 mm; then r is chosen so that a one standard deviation error corresponds to the track being translated along its tangent vector from its distance of closest approach to the 5 mm cylinder radius. This prevents the formation of accidental vertices for tracks which appear to cross far from the

beam axis and at the same time allows tracks to move along the tangent vector for reasonable distances in the vertex finding procedure.

We next order the tracks according to weights which express the information quality for vertex finding. Since the two B's typically have very similar x and y coordinates but different z coordinates, we use as the weight the value of $\frac{\sin\theta}{\sigma}$ where θ is the angle between the track and the z axis. This gives larger weight to the tracks which have better resolution in the z direction.

As a measure of how well a set of tracks forms a single vertex, we define a χ^2 for the set of tracks. In general, for any number of tracks indexed by k the vertex location $\vec{x}_V$ and associated χ^2 deviation are calculated by minimizing

$$\chi^2 = \sum_k (x_k^i - x_V^i)(M_k^{-1})_{ij}(x_k^j - x_V^j) \ .$$

For two tracks from the same vertex, we expect this χ^2 to correspond to one degree of freedom assuming the vertex is well inside the 5 mm cylindrical fiducial region discussed above.

The vertex finding begins as follows: for each track we form in turn a two track vertex with every track of higher weight. If all such vertices have a χ^2 corresponding to greater than about 2.5 standard deviations, the track being examined is added to the set of tracks, called lead tracks, which come from distinct vertices.

The next step is to assign the remaining tracks to the various vertices. This is done by assigning each track to the vertex containing the lead track which has the smallest two-track χ^2 with the given track. Finally, after all tracks have been assigned in this way, the multi-track vertex locations and χ^2 are calculated from the full set of tracks assigned to each vertex.

This procedure occasionally gives a large multi-track χ^2 even though each individual track paired with the lead track gives an acceptable χ^2. For cases where the multi-track χ^2 probability is less than about 0.3%, the initial vertex

is split into two vertices. This is done by forming a plane which is normal to the lead track tangent vector through the initial vertex location. The two new vertices are calculated from the tracks whose closest approach to the lead track lies above or below this plane, respectively. The lead track is then assigned to the vertex to which it comes closer.

The track position errors and particle lifetimes are such that in only a small fraction of the events are all vertices found with all particles correctly assigned. Therefore, the vertex finding is most useful when combined with external particle identification and kinematic information. In the physics discussion below, one B decay will in fact be fully reconstructed using information mostly external to the vertex detector. The vertex information is then crucial for measuring the position of the second B meson. We summarize the quality of the vertex information for this case:

Fraction of B decays with only one vertex found	61%
Fraction of B decays with two vertices found	31%
Fraction of B decays with three or more vertices found	8%
Transverse position error for chosen primary B vertex	20 μm
z position error for chosen primary B vertex	30 μm
For B decays with two vertices and a lepton of momentum > 800 MeV/c in the center of mass, fraction of time primary B vertex is correctly identified	86%

5. Analysis Procedure

In order to measure CP violation, we must identify events in which one B meson decays to a CP eigenstate (such as $J/\psi K_S^0$) and the other decays to a final state which identifies the B meson as a B^0 or $\overline{B}^0$. The latter B will be referred to as the tagging B. The relative decay position of the two B's must be measured to observe a CP violating effect.

In this analysis, we will concentrate on the CP eigenstate $J/\psi K_S^0$ with the J/ψ decaying to a lepton pair. Then the vertex position of the lepton pair gives the decay position of the B decaying to a CP eigenstate. Since the B mesons are produced almost at rest in the $\Upsilon(4S)$ system, the two B's will have almost the same decay position in the plane perpendicular to the beam direction even in the laboratory frame. Therefore, the J/ψ vertex position in this plane can also be used to identify the primary decay products of the tagging B. This is illustrated in Fig. 6. The difference in decay position along the beam direction between the J/ψ vertex and the primary vertex for the tagging B then measures the relative time between decays $t = t_2 - t_1$ referred to in the previous section.

We use charged K's or charged leptons to identify the tagging B as a B^0 or $\overline{B}^0$. Throughout this analysis we assume perfect particle identification. However, we will discuss the background levels which would result from particle misidentification. We impose the following fiducial cuts on all charged tracks: they must have $p_T \geq$100 MeV, and $|\cos\theta| \leq 0.98$ (in the laboratory frame). Where appropriate, we will discuss the effects of relaxing or tightening these requirements. We have not made use of any constrained fits in this analysis.

5.1 RECONSTRUCTING THE J/ψ

In order to test the analysis, we use 2000 simulated $B^0\overline{B}^0$ events in which one of the B's decays to $J/\psi K_S^0$, and the J/ψ decays leptonically. If we assume a branching fraction of 5×10^{-4} for $B \rightarrow J/\psi K_S^0$, and a J/ψ leptonic branching ratio of 14%, this represents 1.4×10^7 $B^0\overline{B}^0$ events. This assumption for the $B \rightarrow J/\psi K_S^0$ branching fraction is based on the measured branching fraction[13] of $(8 \pm 3) \times 10^{-4}$ for $B^{\pm} \rightarrow J/\psi K^{\pm}$.

Since the extreme cleanliness of this decay mode is due to the clear signature of the J/ψ decaying to an oppositely charged pair of leptons, our first step is to try and reconstruct this state. We accept any e^+e^- or $\mu^+\mu^-$ pair whose invariant mass is between 3.0 and 3.2 GeV to be a J/ψ candidate. We then accept the J/ψ

candidate if the leptons form a single vertex with a $\chi^2 \leq 12$ for the vertex fit. The resolution on the position of the J/ψ vertex is 17 μm in the transverse direction, and 20 μm in the z direction. We find at least one J/ψ candidate which satisfies all of the above selection criteria in 90% of the events. In about 1% of the events, we find more than one candidate; this ambiguity is resolved later.

We have assumed that we can identify both electrons and muons over the full range of momenta from J/ψ decays; *i.e.*, 0.4 GeV/c to 6.5 GeV/c. Electrons pose no problem; muons may be more of a challenge in the low momentum range. Čerenkov counters and dE/dx can provide μ/π separation up to a momentum of about 500 or 600 MeV/c; a combination of muon range chambers and coarser muon counters and absorber can probably cover the rest of the range. If, for example, muons cannot be identified in the 500 to 800 MeV/c range, about 6% fewer $J/\psi K_S^0$ events are reconstructed.

5.2 Reconstructing the K_S^0

The next step is to find a K_S^0 either in the $\pi^+\pi^-$ or $\pi^0\pi^0$ decay mode. For the easier (and dominant) charged mode, we simply calculate the invariant mass of all pairs of oppositely charged pions. We accept any pair whose mass is between 480 and 515 MeV. We then accept the K_S^0 candidate if the pions form a single vertex with a $\chi^2 \leq 12$ for the vertex fit. We could further purify the K_S^0 sample by requiring that the vertex position be displaced radially from the beamline; however, we have not found it necessary to actually invoke this cut for finding the B. We find on average 1.0 K_S^0 candidates per event in the $\pi^+\pi^-$ mode.

To reconstruct the neutral mode, we first select neutral showers which meet the following criteria: energy$\geq$30 MeV, $|\cos\theta| \leq 0.99$, and no other charged or neutral particle within 25 milliradians. More than 99% of the photons which pass the first two cuts also pass the third (this fraction drops to 97% if this cut is increased to 50 milliradians). We then form the invariant mass of each pair of photons. Any pair whose mass is between 100 and 170 MeV, and whose opening angle is $\leq 90^\circ$ is considered as a π^0 candidate.

We then calculate the invariant mass of each pair of π^0 candidates, after checking that the two pions are made of four distinct photons (since one photon may be used by more than one π^0 candidate). We accept as a K_S^0 candidate any $\pi^0\pi^0$ combination whose mass is between 465 and 530 MeV. We find on average 2.9 K_S^0 candidates per event in the $\pi^0\pi^0$ mode; many of these are due to wrong photon combinations and our loose cuts. Adding the further requirement that the K_S^0 have $p_T \geq 250$ MeV/c eliminates some of the wrong combinations. It also eliminates some real K_S^0's, but none from the $B \to J/\psi K_S^0$ decay. After this last cut, about 2.3 K_S^0 candidates remain per event in the $\pi^0\pi^0$ mode.

5.3 Reconstructing the B from the $J/\psi K_S^0$

Once the J/ψ('s) and K_S^0('s) have been found, we calculate the invariant mass of each combination in the event. This invariant mass distribution is shown in Fig. 7 for all the $J/\psi K_S^0$ candidates. We boost the $J/\psi K_S^0$ combination back to the Υ(4S) rest frame to determine the total momentum p_{cm} of the $J/\psi K_S^0$ combination in this frame. A combination is defined to be a B candidate if $p_{cm} \leq 450$/c MeV, and the reconstructed mass of the combination lies between 5.15 and 5.45 GeV. (We cut more tightly on the lower edge of the mass region in order to eliminate background from $B \to J/\psi K_S^0 \pi^0$ which has opposite sign CP; we will discuss this in more detail below.) We find at least one combination that meets these criteria in 61% of the events. If we require that all charged and neutral particles have $|\cos\theta| \leq 0.95$, this drops to 48%; it drops even further, to 23%, if we cut at $|\cos\theta| \leq 0.90$. This clearly demonstrates the need for good forward particle detection, down to within 10° of the beamline.

In about 3% of the events, we find more than one combination which passes the selection criteria. Note that choosing the correct K_S^0 is actually unimportant, as long as our cuts are not so loose that they allow background events from other processes. However, the correct choice of J/ψ candidate is very important since the J/ψ candidate determines the vertex positions of the B mesons. These multiple combination ambiguities are resolved in the following way. First, if the

combinations involve different J/ψ candidates, we select the J/ψ candidate with the smaller total χ^2, where the total χ^2 is the sum of the vertex χ^2 and the mass χ^2. Secondly, if the combinations involve different K_S^0 candidates, we form a total χ^2 for the B candidate by adding its mass χ^2 and its "momentum χ^2", where the momentum χ^2 is defined as the square of the ratio (p_{cm}(measured) - p_{cm}(expected))/(resolution). The candidate with the best total χ^2 is chosen.

In fact, in the 1210 reconstructed events, there was no J/ψ ambiguity in any event after forming the B candidates. In one event the ambiguity involved two possible $K_S^0 \to \pi^+\pi^-$, and in this case it was resolved correctly. In 49 events, the multiple $B \to J/\psi K_S^0$ candidates involved two or more possible $K_S^0 \to \pi^0\pi^0$. In 63% of the events, the correct choice was made (*i.e.*, the correct four photons were used to construct the K_S^0 used for the B). In the other 37% of the events, the K_S^0 that was used was constructed from three out of four (14 events) or two out of four (4 events) of the correct photons, plus one or two other photons.

5.4 Finding the Vertex of the Tagging B

Once a $B \to J/\psi K_S^0$ candidate has been identified, we group all the charged tracks in the event into vertices ignoring the leptons from the J/ψ candidate and the pions from the K_S^0 candidate. However, we add one track calculated from the vertex parameters of the J/ψ candidate. As explained above, the primary vertices of the two B's will be very close to each other in the plane transverse to the beam direction. The separation of the two vertices in the transverse plane is determined by the transverse momenta and the lifetimes of the B's. We use the measured transverse momentum of the $J/\psi K_S^0$ candidate and the mean B lifetime to translate the measured J/ψ vertex to the mean position of the primary vertex for the tagging B in the transverse plane. When grouping tracks into vertices, we assume that the position along the beam direction of the translated J/ψ vertex is unknown. The vertex which contains this translated J/ψ track is assumed to be the primary vertex of the tagging B.

5.5 THE TAGGING B

We now need to identify the tagging B as a B^0 or a $\overline{B}^0$. Two techniques have been used: lepton tagging, which uses semileptonic decays of the B, and charged kaon tagging, which uses charged K's from the *bottom* $\rightarrow$ *charm* $\rightarrow$ *strange* cascade. The sign of the electric charge of the lepton or K identifies the B as a B^0 or $\overline{B}^0$.

Lepton Tagging

To correctly identify the tagging B as a B^0 or $\overline{B}^0$, we must select leptons from the primary decay of the B meson. These leptons tend to have higher momentum in the B rest frame than leptons from secondary decays such as the decay of the charm quark. We boost the momentum of each lepton back into the $\Upsilon(4S)$ rest frame. This momentum is shown in Fig. 8a and 8b for right-sign and wrong-sign leptons, respectively. (A right-sign lepton is defined as one whose electric charge corresponds to the charge of a lepton from the primary decay of the B^0 or $\overline{B}^0$.) We accept any lepton with momentum in the $\Upsilon(4S)$ rest frame greater than 1.4 GeV. There is very little contamination from wrong-sign leptons in this sample. In addition, we accept leptons with momentum between 0.8 and 1.4 GeV if exactly two vertices are found for the tagging B and the lepton belongs to the same vertex as the J/ψ vertex (*i.e.*, the primary vertex). Of the leptons with momentum between 0.8 and 1.4 GeV, about 36% satisfy this vertex requirement. Events with only one lepton satisifying the above criteria are accepted as tagged events. The total tagging efficiency is 14% with 94% of the tags correct.

Kaon tagging

Besides the cascade decay which can lead to a charged kaon useful for tagging, we must consider other sources of charged K's in B decays. The Cabibbo-allowed decay $B \rightarrow D_s\overline{D}X$ can result in a wrong-sign kaon; it is likely to be accompanied by one or more other charged or neutral K's, however. In events with a single charmed meson, the Cabbibo-suppressed decays will generally result in two kaons

(either oppositely charged, one wrong-sign charged and one neutral, or both neutral), or no kaons at all. Doubly-Cabibbo-suppresed decays of the charm meson (which fortunately are relatively rare) can give a single wrong-sign K. Cabibbo-suppressed decays of the B can add a kaon of the right sign.

Hence we accept two cases. If there are two charged kaons of the same sign (including the case when there are a total of three charged K's) we accept that sign as tagging the B. If there is a single charged K, and no good $K^0_S \to \pi^+\pi^-$ candidates (other than the one from the $B \to J/\psi K^0_S$ candidate), we again accept the charged K as a good tag. This method tags 40% of the events containing a $B \to J/\psi K^0_S$ candidate (37% with a single K, 3% with two or three K's), with 92% of the tags being correct.

Combined tagging

There is some overlap of the two tagging methods. In the 5% of events where both tags are available, they agreed on the identity of the B meson as a B^0 or $\overline{B}^0$ 92% of the time (the five events in which they disagreed were considered untagged). Overall, we tag 48% of the events containing a $B \to J/\psi K^0_S$ candidate with 92% of the tags being correct. The combined reconstruction and tagging efficency is $29 \pm 1\%$. The efficiency for tagging is less sensitive to the track $|\cos\theta|$ cut than is the $B \to J/\psi K^0_S$ reconstruction efficiency. It drops from 48% for $|\cos\theta| \leq 0.98$ to 44% for $|\cos\theta| \leq 0.95$, and to 39% for $|\cos\theta| \leq 0.90$.

5.6 Backgrounds to $B \to J/\psi K^0_S$ Reconstruction

Although the $B \to J/\psi K^0_S$ signature is very distinctive, the branching fraction is relatively small ($\approx 5 \times 10^{-4}$). Therefore, this mode could have significant backgrounds. We have investigated three possible sources of background: events in which a hadron is misidentified as a lepton to form a J/ψ candidate, events in which both B's decay semileptonically, and events in which $B \to J/\psi K^0_S \pi^0$, a process which can also be used for measuring CP violation but which has opposite sign CP and therefore must be well separated from $B \to J/\psi K^0_S$.

Particle Misidentification We generated a variety of events, including events in which one or both B mesons decay semileptonically, and associated the leptons with pions in the event to attempt to reconstruct a J/ψ candidate. We find no candidates for $B \rightarrow J/\psi K_S^0$ resulting in an estimate of less than 2.0% background at the 90% confidence level for a particle misidentification probability of 1%.

Events with two semileptonic decays

Since the branching ratio for $B \rightarrow e^{\pm}X$ and $B \rightarrow \mu^{\pm}X$ are each roughly 12%, we expect the rate for same-flavor double semileptonic events to be almost 3%, about 400 times larger than the $B \rightarrow J/\psi K_S^0$, $J/\psi \rightarrow l^+l^-$ rate per event. In order to measure the background from this process, events with two semileptonic B decays were generated at random. A preselection was then done to choose only those events in which same-flavor opposite sign leptons had an invariant mass within 200 MeV of the J/ψ mass, and in which there was at least one K_S^0. In order to get 2000 such events, over 121,000 double semileptonic events were generated. Thus the 2000 events represent 2.2 million $B^0\overline{B}^0$ events. None of these events pass our selection criteria for a $B \rightarrow J/\psi K_S^0$ candidate. The $J/\psi K_S^0$ invariant mass plot is shown in Fig. 9. Normalizing to the number of events in the signal channel, we estimate a background from double semileptonic decays of less than 1.5% at the 90% confidence level. We estimate that events in which one B decays semileptonically, and then the charm state also decays semileptonically, produce fake J/ψ's at only 10% to 20% of the rate for events in which both B's decay semileptonically.

$B \rightarrow J/\psi K_S^0 \pi^0$

We expect the product branching ratio[13] for $B \rightarrow J/\psi K^{*0}$, $K^{*0} \rightarrow K_s^0\pi^0$ to be about equal to the $B \rightarrow J/\psi K_S^0$ rate. Thus we simulated 2000 events in which one B decays to $J/\psi K^{*0}$ and every K^{*0} decays to $K_S^0\pi^0$. Only 18 events pass our selection criteria for $J/\psi K_S^0$ candidates. The invariant mass of the $J/\psi K_S^0$ candidates is shown in Fig. 10 before our final B mass cut. The background rate is primarily a function of the detector's mass resolution, which in turn is a

function of the momentum resolution of the tracking chambers and the energy resolution of the calorimeter. These 18 events represent a background of less than 1.5% which is not significant.

5.7 Backgrounds to Tags

There are two possible reasons for incorrectly tagging the B as a B^0 or $\overline{B}^0$. First, the charged lepton or kaon may be correctly identified but nevertheless have the wrong sign because of secondary or Cabibbo-suppressed decays. As mentioned above, this background is about 6% for the lepton tag and 8% for the kaon tag. Secondly, a wrong-sign particle may be misidentified as a lepton or kaon. The particle misidentification probability should be low enough such that the background from the second source is significantly less than the background from the first source.

Misidentifying a charged kaon as a lepton does not introduce a background to the lepton tag because most charged kaons which pass the momentum cuts used for lepton tagging have the same sign as the lepton from primary B decay. It was determined that the number of wrong-sign charged pions and the number of right-sign leptons which meet the selection criteria for a lepton tag are about the same in events with a reconstructed $B \rightarrow J/\psi K_S^0$ candidate. Therefore, if the probability of misidentifying a pion as a lepton is less than about 2%, this background to the lepton tag will be less than half of that due to wrong-sign leptons.

As stated previously, 8% of the charged kaon tags are actually of the wrong sign. Since we find a $K^{\pm}$ tag in 40% of the reconstructed events, this produces 3.2% wrongly tagged events. In addition, if we ignore charged pions from K_S^0 decays, there are an average of 1.7 wrong-sign pions per event. This means for every 1% probability of misidentifying a pion as a kaon, we would have an additional 1.7% wrongly tagged events. This indicates that the K/π misidentification rate must be kept to $\sim$1% for momenta up to 3 GeV/c to prevent the misidenti-

fied pions from dominating our mistagging rate. A Čerenkov ring-imaging device would probably be required.

It should be noted that if one is not able to obtain such a low misidentification rate with high efficiency for kaons, one could instead use D tagging. We estimate that by using D mesons (reconstructed in their simpler decay modes, such as $K^+\pi^-(\pi^0)$, $K^+\pi^-\pi^-(\pi^0)$, $K^+\pi^-\pi^+\pi^-$, $K^0_S\pi^-$, etc.), together with the lepton tags, 30% of the events can be tagged with only 5% wrong tags.

5.8 Correction to Measured Asymmetry due to Backgrounds

Although the backgrounds dilute the measured asymmetry, the effect is fully correctable if we can accurately estimate the size of each background. In general, the measured asymmetry A_{meas} is related to the true asymmetry A_{true} by the relation

$$A_{meas} = A_{true}(1 - 2P)$$

where P is a measure of the fraction of the sample which is background. For example, for backgrounds due to wrong-sign lepton or kaon tags, P is the probability that a tag has the wrong sign. As stated above, this probability is about 6% for the lepton tag and 8% for the charged kaon tag. For backgrounds due to misidentified lepton or kaon tags, P is the particle misidentification probability per event times the ratio of untagged to tagged events. For the analysis outlined above, the ratio of untagged to tagged events is about one.

The size of backgrounds to tags can be estimated from the data itself using pairs of charged B mesons. Since the charged B mesons cannot mix, the only sources of two like-sign tags in an event are secondary decays and particle misidentification. Since the statistical error on A is expected to be about 0.03 for 1000 tagged events, and A is expected to be in the range 0.1 to 0.3 in the Standard Model, we would like to know the correction to A_{meas} due to backgrounds to significantly better than 10%. Since the corrections themselves are generally not larger than 10%, this should not pose a problem.

In order to minimize the statistical error in the asymmetry measurement, the tagging strategy must be optimized. This requires balancing high tagging efficiency against a higher percentage of incorrect tags. This optimization would depend on the size of the data sample and the precision required. While fairly "loose" tagging would be very useful in an initial search with a small data sample, cleaner, less efficient methods might be preferable for larger data sets and higher precision.

In Table 1, we summarize the number of events generated for this analysis, the assumed branching fractions and the size of the equivalent $B^0\overline{B}^0$ data sample, the charged and neutral track geometrical criteria, the number of $B \to J/\psi K_S^0$ candidates and, finally, the number of tagged events. For B decay to the CP eigenstate $J/\psi K_S^0$, the size of the final correctly tagged sample is 533 events for 1.4×10^7 produced $B^0\overline{B}^0$ pairs.

5.9 Measuring CP Violation

To finally measure CP violation, we use the time-ordering of the decays determined by the relative positions of the J/ψ vertex and the tagging B vertex along the beam direction and the identity of the tagging B from the $K^{\pm}$ or lepton tag to divide the events into the four categories described in section 2.1 (B^0 first, $J/\psi K_S^0$ second; $J/\psi K_S^0$ first, B^0 second; $\overline{B}^0$ first, $J/\psi K_S^0$ second; $J/\psi K_S^0$ first, $\overline{B}^0$ second). Combining the first and fourth categories, and the second and third categories, we plot the Δz distribution (the difference in position of the J/ψ vertex and the tagging B vertex along the beam direction, which is proportional to the relative decay-time, to a good approximation). The resolution on Δz is shown in Fig. 11, where the difference between the true (generated) Δz and the measured Δz is histogrammed for all reconstructed events (tagged and untagged). Given 577 reconstructed and tagged events, we find an asymmetry in the number of events of 0.05 ± 0.04. If $\Delta m/\Gamma = 0.75$, this translates into a

Table 1. Summary of results for the CP eigenstate $J/\psi K_S^0$.

Number of generated events with one			
$B \to J/\psi K_S^0$ decay	2000		
Assumed branching fractions for:			
$B \to J/\psi K_S^0$	5×10^{-4}		
$J/\psi \to l^+ l^-$	0.14		
Equivalent number of produced $B^0\overline{B}^0$ pairs	1.4×10^7		
Charged track criteria:			
minimum transverse momentum	0.1 GeV/c		
maximum $\lvert\cos\theta\rvert$	0.98	0.95	0.90
Neutral track criteria:			
minimum energy	0.03 GeV		
maximum $\lvert\cos\theta\rvert$	0.99	0.95	0.90
Number of $B \to J/\psi K_S^0$ candidates	1210	870	452
Number of right-sign lepton tags	159	109	55
Number of wrong-sign lepton tags	11	9	6
Number of right-sign kaon tags	438	300	127
Number of wrong-sign kaon tags	38	32	14
Total number of right-sign tags	533	368	169
Total number of wrong-sign tags	44	38	18

measurement of $\sin 2\phi$ of 0.10 ± 0.08 using this integrated asymmetry only. We can do better by performing a simultaneous fit to the two time distributions to derive $\sin 2\phi$ itself; this reduces the error to ± 0.07; the fit is shown in Fig. 12. Known values of $\Delta m/\Gamma$ and the B^0 lifetime are input to the fit; these will be well measured by the time this measurement is attempted. For our sample of 2000 events in which one B meson decays to $J/\psi K_S^0$, we measure $\sin 2\phi$ to be $0.06 \pm$

0.07, consistent with no CP violation, as was the case for the generated events.

For a second, similar sample of 2000 events, we measure an event asymmetry of -0.19 ± 0.04. After correcting for the dilution due to wrong sign tags, this becomes -0.22 ± 0.05. This translates into $\sin 2\phi = -0.46 \pm 0.10$; fitting the time distributions (Fig. 13) yields the value -0.41 ± 0.06, in good agreement with the value of -0.40 which was used to generate the events. We have also carried out a parallel analysis of 2000 $B \to J/\psi K^{*0}, K^{*0} \to K^0_S \pi^0$ events. In this case, a fit to the time distributions (Fig. 14) yields $\sin 2\phi = 0.45 \pm 0.07$, which is also in good agreement with the input value of 0.40.

6. Conclusions

6.1 Detector Requirements

In order to achieve this type of measurement a very good detector, with a geometry adapted to the asymmetry of the events, would be needed. Since vertex detection is critical, it is important that the radius of the beampipe be no more than 1.5 cm. Surrounding the beampipe, an excellent high resolution ($\sigma \approx 10$ μm) vertex detector (CCD's or another silicon pixel technology) is required. The vertex detector should extend about 30 cm in the forward direction, and out to a radius of approximately 10 cm. Since it is also important to minimize multiple scattering, only a few layers of silicon should be used. These would take the form of a barrel in the central region, plus several planes perpendicular to the beamline in the forward direction. Around the vertex detector would be a high resolution ($\sigma \approx 100$ μm) drift chamber. The momentum resolution should be at least $\frac{\sigma_{p_T}}{p_T} = 0.005 p_T$ (p_T in GeV/c). The tracking chambers might take either of two forms. One could use a fairly small conventional cylindrical central chamber (roughly 1.2 meters long), with 50 to 60 layers of sense wires, plus a forward tracking chamber with 100 to 120 tracking planes perpendicular to the beamline. Alternatively, a single, long (~3.5 meters) cylindrical chamber,

placed so that two-thirds of it extended in the forward direction could be employed. In either case the chamber(s) should include the capability of making dE/dx measurements. In order to keep the detector compact, a relatively high magnetic field of $\sim$ 1.5 tesla would be needed. This could easily be supplied by a superconducting coil (surrounding the electromagnetic calorimetry).

Outside the tracking chambers, in the central and forward regions, ring-imaging Čerenkov counters, using NaF crystal radiators, could provide the necessary kaon identification for momenta up to 3 GeV/c. As described in reference 14, such counters require a space of 10 to 20 cm for the opening of the Čerenkov cone. This would be followed by electromagnetic calorimetry; NaI or BGO crystals could provide the required photon and electron energy resolution of $\frac{\sigma_E}{E} = \frac{0.02}{\sqrt[4]{E}}$ (E in GeV).

We would like to be able to identify muons at momenta as low as $\sim$ 400 MeV/c in order to reconstruct J/ψ's. The Čerenkov counters and dE/dx could provide this information up to only about 600 MeV/c. By incorporating muon range chambers in the flux return iron, the momentum range from $\sim$ 600 to $\sim$ 1200 MeV/c could be covered. Coarser layers of detectors and absorber could then provide muon identification at higher momenta. Time-of-flight counters could be placed between the Čerenkov counters and the calorimetry, to provide some redundancy for the particle identification. This combination of detectors could probably provide the momentum and energy resolution and particle identification required, down to small angles ($\cos\theta = 0.98$ or $\sim 10°$) in the forward direction. Such a detector is described in more detail in the 1988 Snowmass Proceedings.[15]

6.2 Required Data Sample

In Table 2, we summarize the total number of events we would expect to reconstruct and correctly tag for three similar CP eigenstate decay modes given 10^7 $B^0\overline{B}^0$ events. We assume that the branching fractions for $B \to J/\psi K_S^0$, $B \to \psi' K_S^0$ and $B \to J/\psi K^{*0}$ with $K^{*0} \to K_S^0\pi^0$, are each 5×10^{-4}. However,

there is some evidence from the ARGUS collaboration[13] that the branching fraction for $B^+ \to \psi' K^+$ is actually about three times that for $B^+ \to J/\psi K^+$. If this proves to be correct, we should triple the estimates for the number of reconstructed and correctly tagged events for $B^0 \to \psi' K^0_S$ given in Table 2.

For both the $\psi' K^0_S$ and $J/\psi K^{*0}$ modes, we assume that the efficiency for correctly tagging the B meson with a lepton or charged kaon is 48%, the same efficiency that we found for the $J/\psi K^0_S$ mode. The reconstruction efficiency for $J/\psi K^{*0}$ is 52% and for $\psi' K^0_S$ is 59% when $\psi' \to l^+l^-$ and 37% when $\psi' \to J/\psi \pi^+\pi^-$. This can be compared to an efficiency of 61% for reconstructing $B^0 \to J/\psi K^0_S$. In every case, only the leptonic decays of the J/ψ are included. We estimate that a combination of these three CP eigenstates would provide a sample of about 1000 reconstructed and correctly tagged events. This would provide a measurement of the CP violating asymmetry with an absolute statistical error of ± 0.03. This translates into an error of 0.06–0.07 on the measurement of $\sin 2\phi$, depending on the magnitude of the $B^0\overline{B}^0$ mixing. As stated earlier, this error can be further reduced by doing a fit to the time distributions.

Table 2. Summary of results for three CP eigenstates with 10^7 produced $B^0\overline{B}^0$ pairs. In every case, only the $J/\psi \to l^+l^-$ mode is included.

Mode		# Produced	# Reconstructed and Tagged
$J/\psi K^0_S$		1400	380
$J/\psi K^{*0}$,	$K^{*0} \to K^0_S \pi^0$	1400	320
$\psi' K^0_S$,	$\psi' \to l^+l^-$	180	50
	$\psi' \to J/\psi \pi^+\pi^-$	470	80
Total		3450	830

Acknowledgements

The authors would like to thank Gary Feldman, Piermaria Oddone and Guy Wormser, along with other members of the SLAC Asymmetric B Factory Working Group, for helpful discussions. We would also like to acknowledge the useful discussions that took place within the e^+e^- B Factory Working Group at the 1988 Snowmass Workshop.

REFERENCES

1. S. L. Wu, *Proceedings of the 1987 International Symposium on Lepton and Photon Interactions at High Energies*, ed. by W. Bartel and R. Ruckl, p. 39 (1988).

2. H. Albrecht *et al., Phys. Lett.* **192B**, 245 (1987). This paper by the Argus collaboration presents a result of $r = 0.21 \pm 0.08$, where r is the mixing parameter. Recently the CLEO collaboration has reported a similar, preliminary result of $r = 0.182 \pm 0.055 \pm 0.056$: N. Katayama, *Proceedings of the Sixteenth SLAC Summer Institute on Particle Physics (July, 1988)*, ed. by E. C. Brennan, to be published.

3. P. Oddone, *Proceedings of the UCLA Workshop: Linear Collider $B\overline{B}$ Factory Conceptual Design*, ed. by D. Stork, p. 243 (1987).

4. I.I. Bigi and A.I. Sanda, *Nucl. Phys.* **B193**, 85 (1981).

5. L. Wolfenstein, *Nucl. Phys.* **B246**, 45 (1984);
   M.B. Gavela *et al., Phys. Lett.* **162B**, 197 (1985).

6. I. Dunietz and J.L. Rosner, *Phys. Rev.* **D34**, 1404 (1986).

7. I.I. Bigi and A.I. Sanda, *Nucl. Phys.* **B281**, 41 (1987).

8. L. Wolfenstein, *Phys. Rev. Lett.* **13**, 180 (1964).

9. I.I. Bigi and A.I. Sanda, *Phys. Lett.* **194B**, 307 (1987).

10. R. Brun *et al.,* CERN DD/EE/84-1 (1987).

11. Review of Particle Properties, *Phys. Lett.* **170B** (1987).

12. See, for example, D.G.Hitlin, CALT-68-1463 (1987).

13. M. S. Alam *et al., Phys. Rev.* **D34**, 3279 (1986);
    H. Albrecht *et al., Phys. Lett.* **199B**, 451 (1987).

14. R. Arnold *et al.,* CERN-EP/87-186 (1987).

15. Report of the e^+e^- B Factory Working Group, *Proceedings of the 1988 Snowmass Summer Study on High Energy Physics in the 1990s*, to be published.

FIGURE CAPTIONS

1. Feynman diagram for semileptonic B decay.
2. Simple vertex detector layout for a machine with $\beta\gamma = 1$ as was used in the simulation.
3. Polar angle distribution of final state particles in the laboratory for a machine with $\beta\gamma = 1$.
4. Momentum spectrum of pions in the laboratory frame.
5. Time between B^0 and $\overline{B}^0$ decays for $\frac{\Delta m}{\Gamma} = 5$ calculated from the distance between decays Δz in the approximation that the B mesons are produced at rest in the center of mass of the event. The solid curve corresponds to the exact time evolution.
6. Example of a $B^0\overline{B}^0$decay illustrating the fact that the two B decay vertices are typically very close together in the plane perpendicular to the beam axis but separated in the direction along the beam axis.
7. Invariant mass distribution for $J/\psi K^0_S$ candidates in events in which one B decays to $J/\psi K^0_S$.
8. Lepton momentum distribution in the Υ(4S) rest frame for (a) right-sign leptons and (b) wrong-sign leptons. The distributions include the effects of finite momentum resolution and limited geometrical acceptance.
9. Invariant mass distribution for $J/\psi K^0_S$ candidates from events with two semileptonic B decays.
10. Invariant mass distribution for $J/\psi K^0_S$ candidates from events in which one B decays to $J/\psi K^{*0}$and $K^{*0} \rightarrow K^0_S\pi^0$.
11. Difference between the true (generated) Δz and the measured Δz, for all reconstructed $J/\psi K^0_S$ events. Δz is the distance between the two primary B decay vertices along the beam axis. The resolution for measuring Δz is approximately 40 μm.

12. The decay length distributions for the two classes of events: (a) first B decays to $J/\psi K^0_S$ and the second is tagged as a B^0, or first is tagged as a $\overline{B}^0$ and second is $B \to J/\psi K^0_S$; (b) first B is tagged as a B^0 and the second is $B \to J/\psi K^0_S$, or the first B decays as $J/\psi K^0_S$ and the second is tagged as a $\overline{B}^0$. No CP violation was included in the generated events.

13. Same distributions as Fig. 12 for the case when CP violation was included in the generated events.

14. Same distributions as Fig. 13 for reconstructed $B \to J/\psi K^{*0}, K^{*0} \to K^0_S \pi^0$ events, when CP violation was included in the generated events.

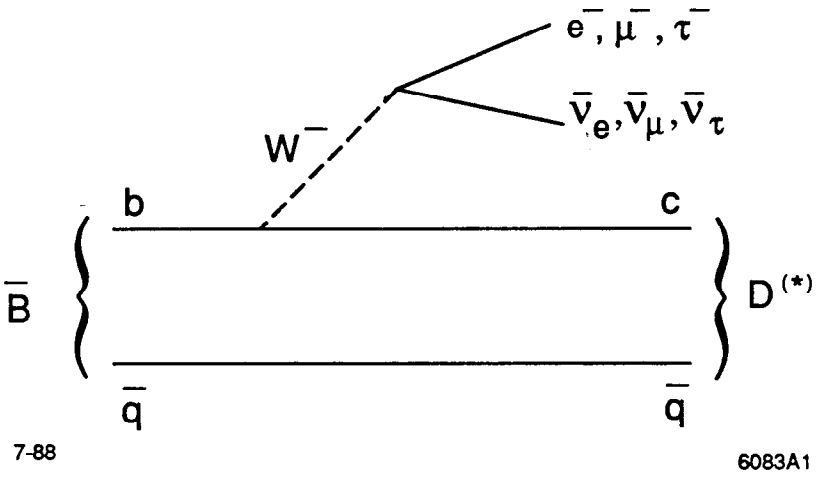

Fig. 1

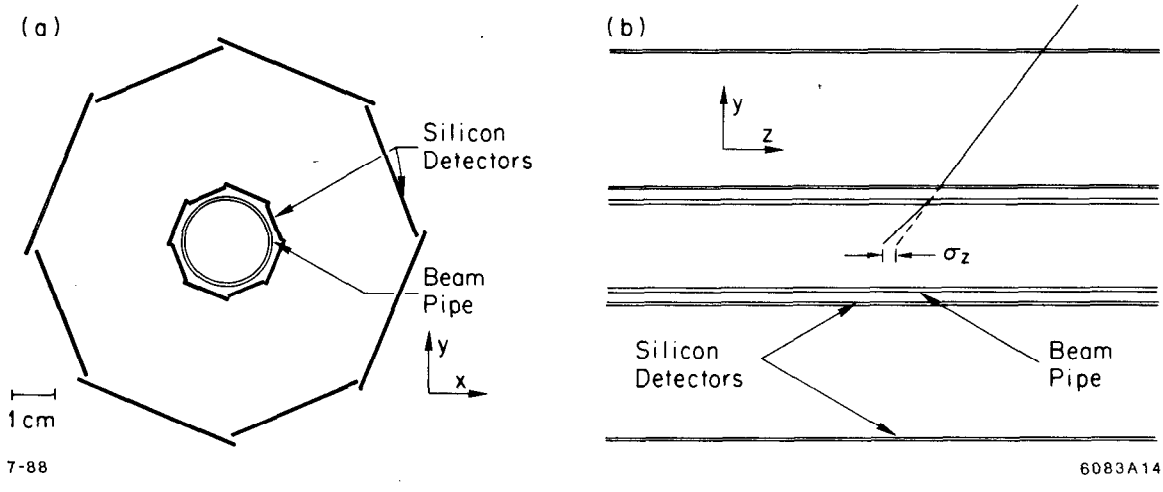
(a)
Silicon
Detectors
Beam
Pipe
y
x
1 cm
7-88
(b)
y
z
σ_z
Silicon
Detectors
Beam
Pipe
6083A14

Fig 2

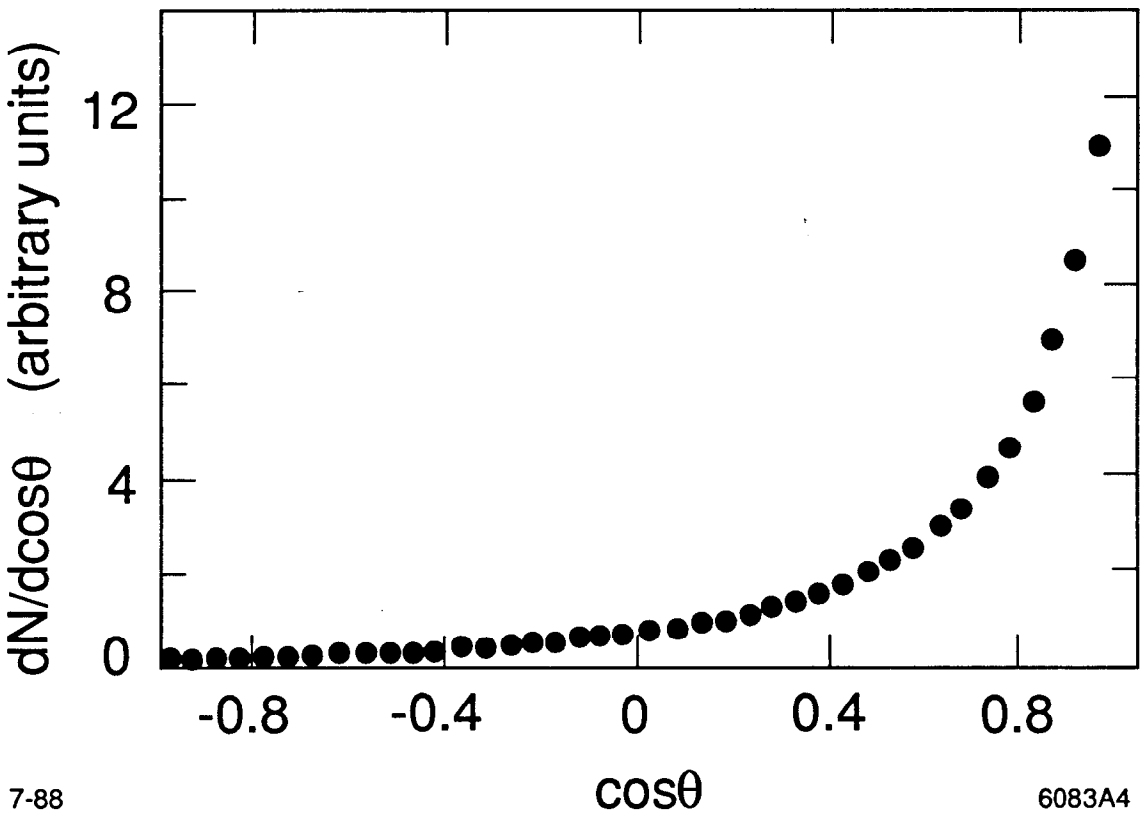

Fig. 3

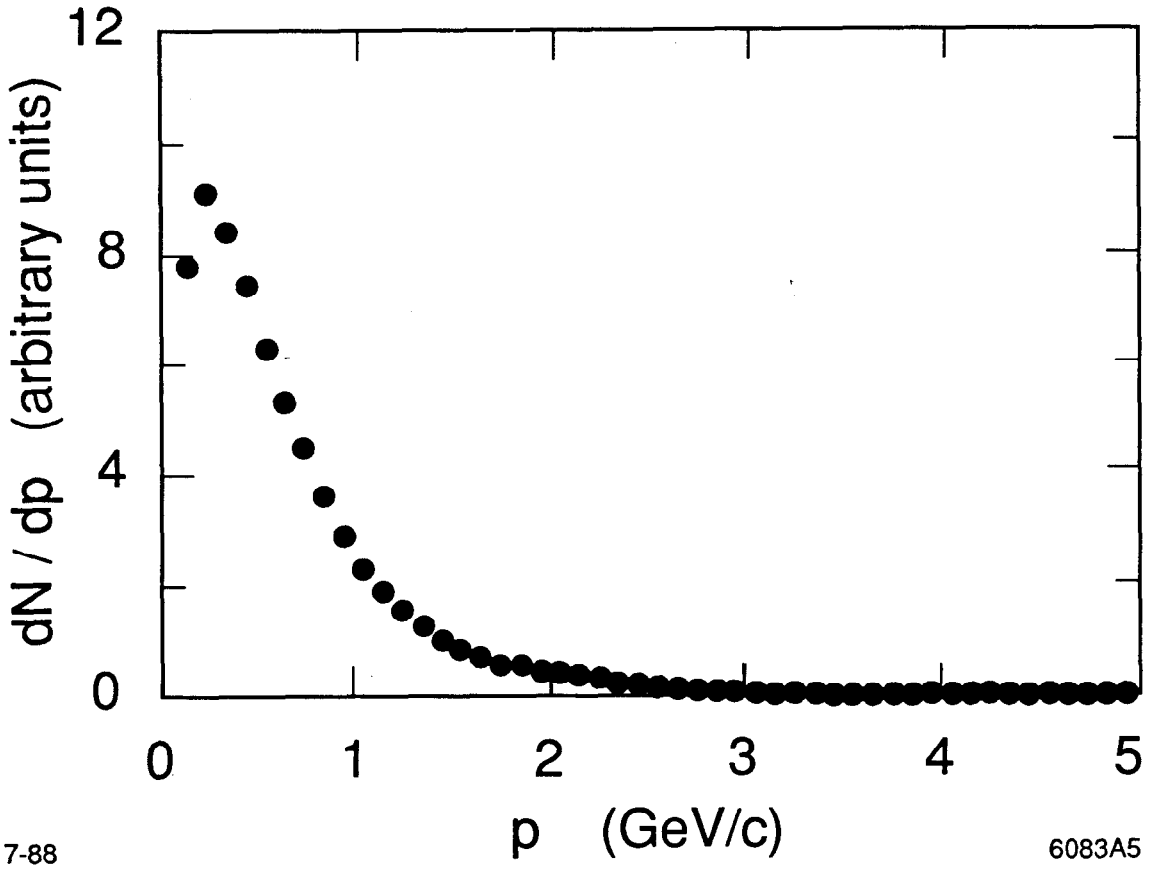

Fig. 4

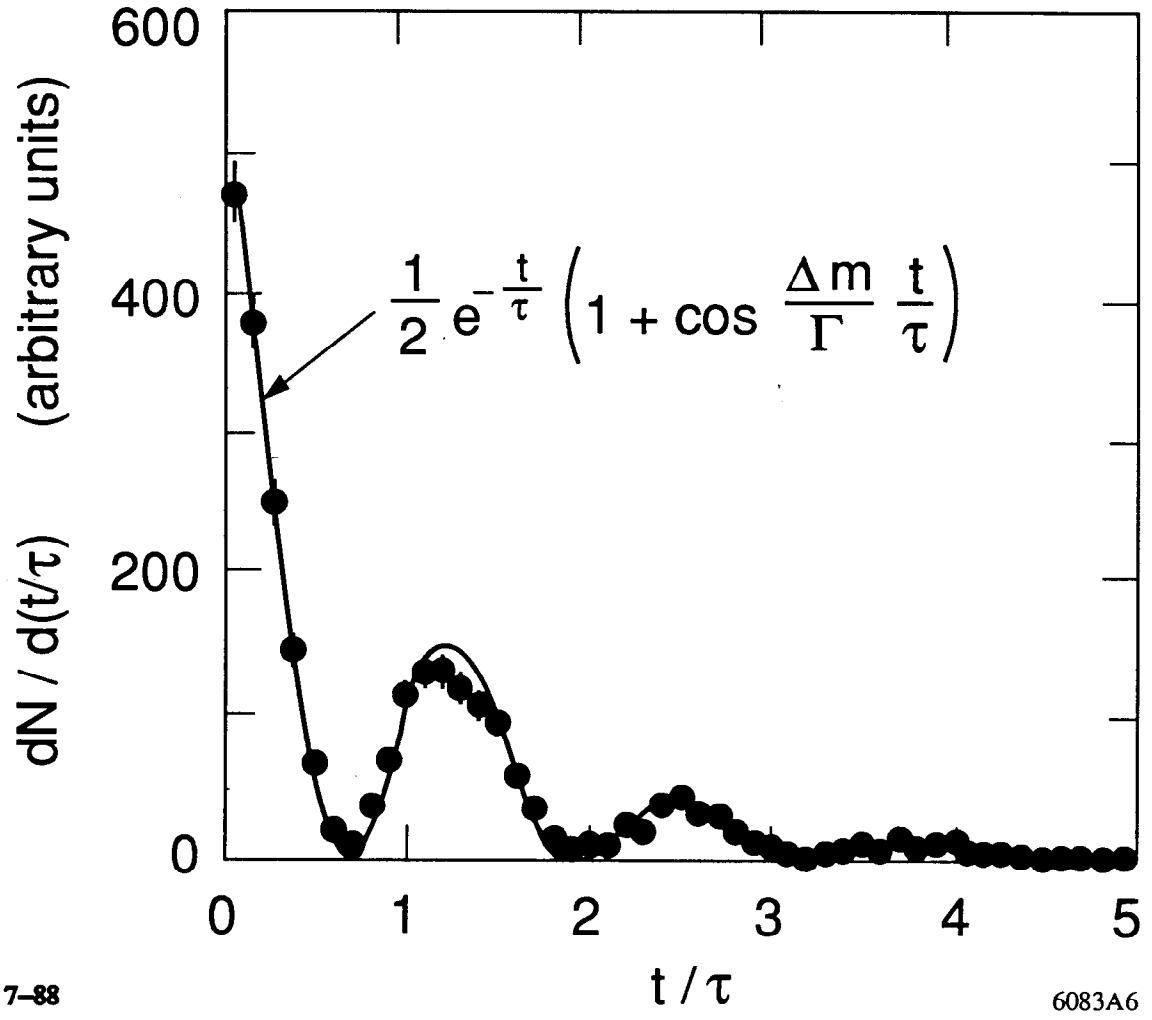
600
400
200
0
dN / d(t/τ) (arbitrary units)
$\frac{1}{2} e^{-\frac{t}{\tau}} \left(1 + \cos \frac{\Delta m}{\Gamma} \frac{t}{\tau}\right)$
0
1
2
3
4
5
t / τ
7-88
6083A6

Fig. 5

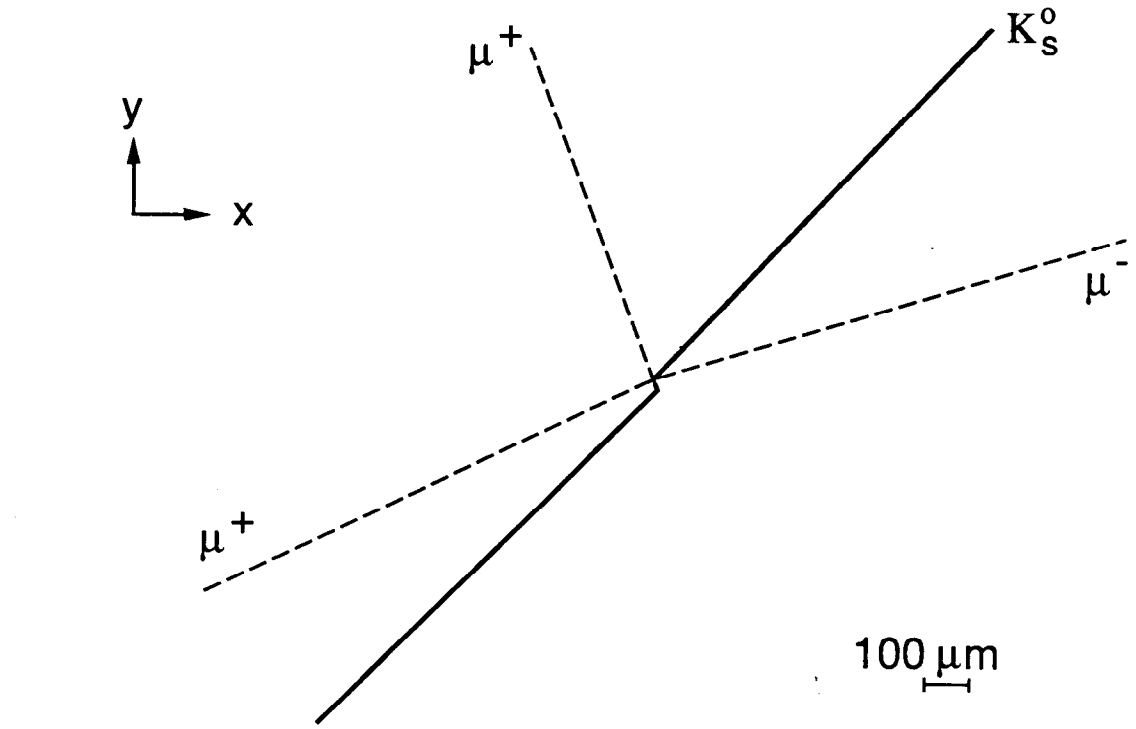
K^o_S
μ^+
y
x
μ^-
μ^+
100 μm

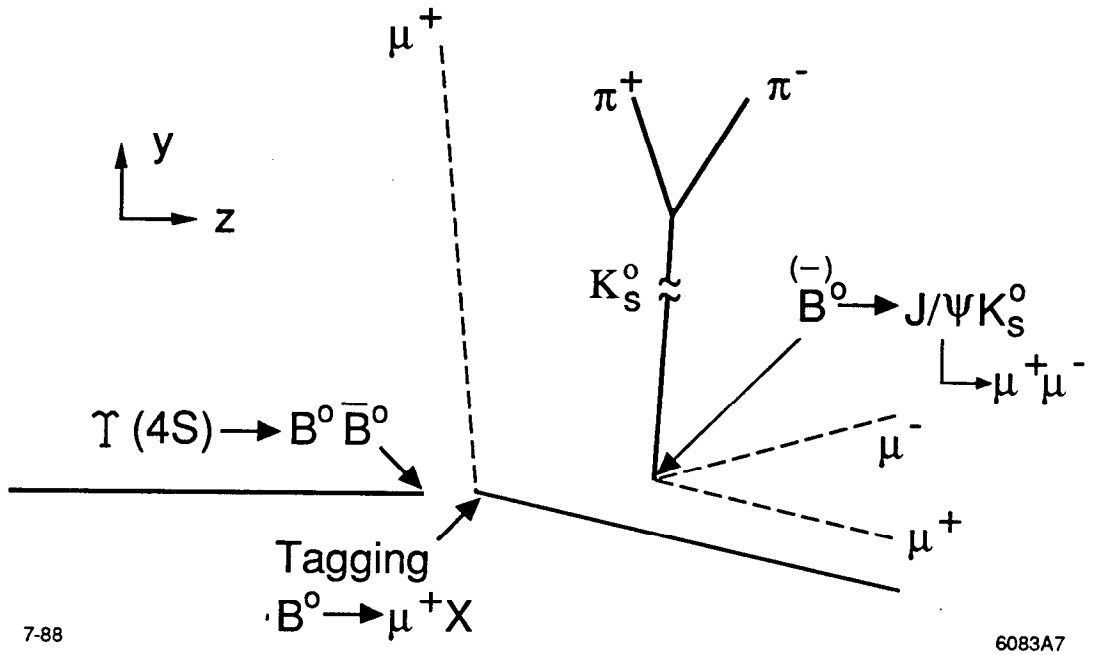
μ^+
π^+
π^-
y
z
K^o_S
$\overset{(-)}{B}{}^o \rightarrow J/\psi K^o_S$
$\mu^+\mu^-$
$\Upsilon(4S) \rightarrow B^o \bar{B}^o$
μ^-
μ^+
Tagging
$B^o \rightarrow \mu^+ X$
7-88
6083A7

Fig. 6

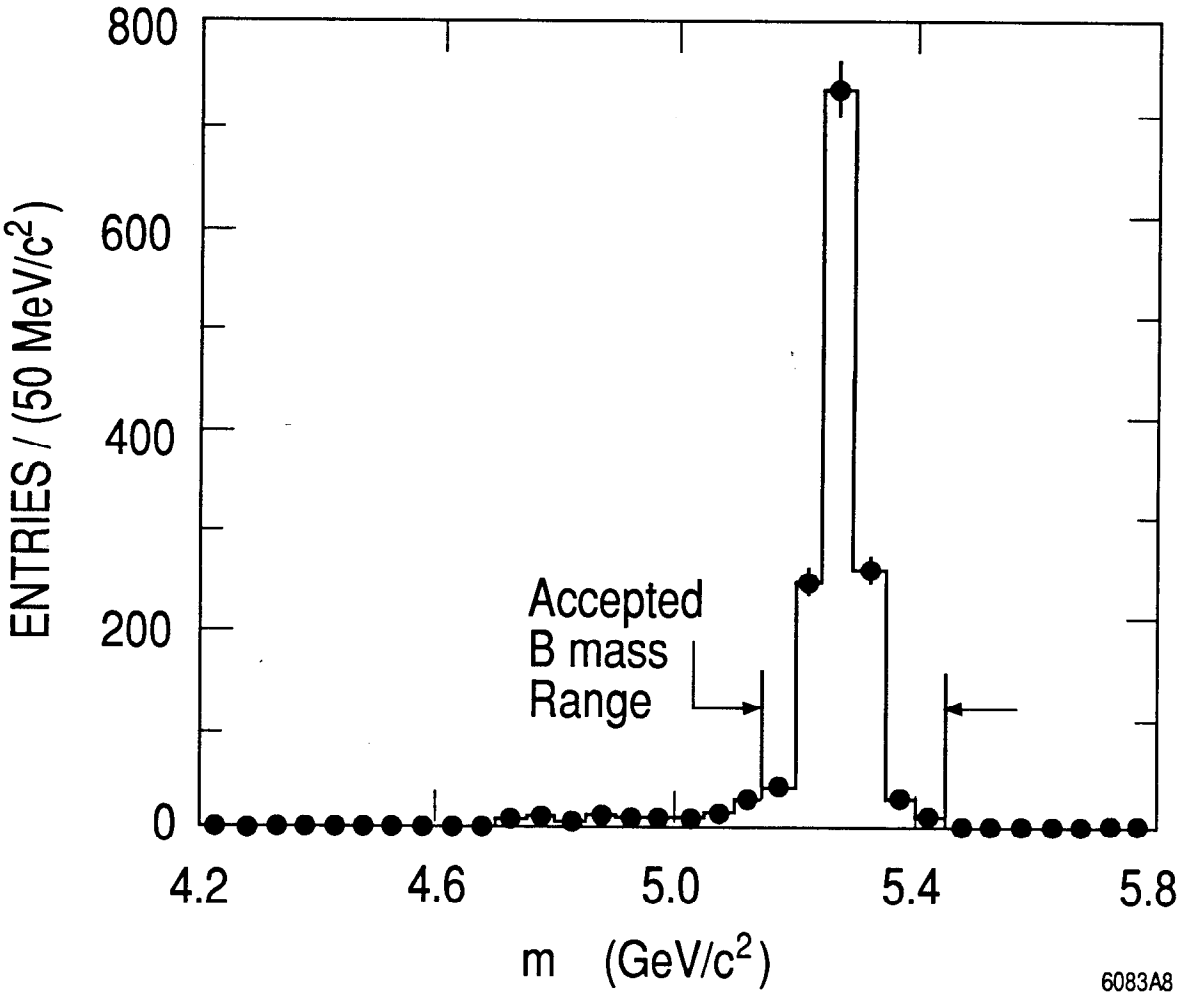
800
600
400
200
0
ENTRIES / (50 MeV/c²)
Accepted
B mass
Range
4.2
4.6
5.0
5.4
5.8
m (GeV/c²)
6083A8

Fig. 7

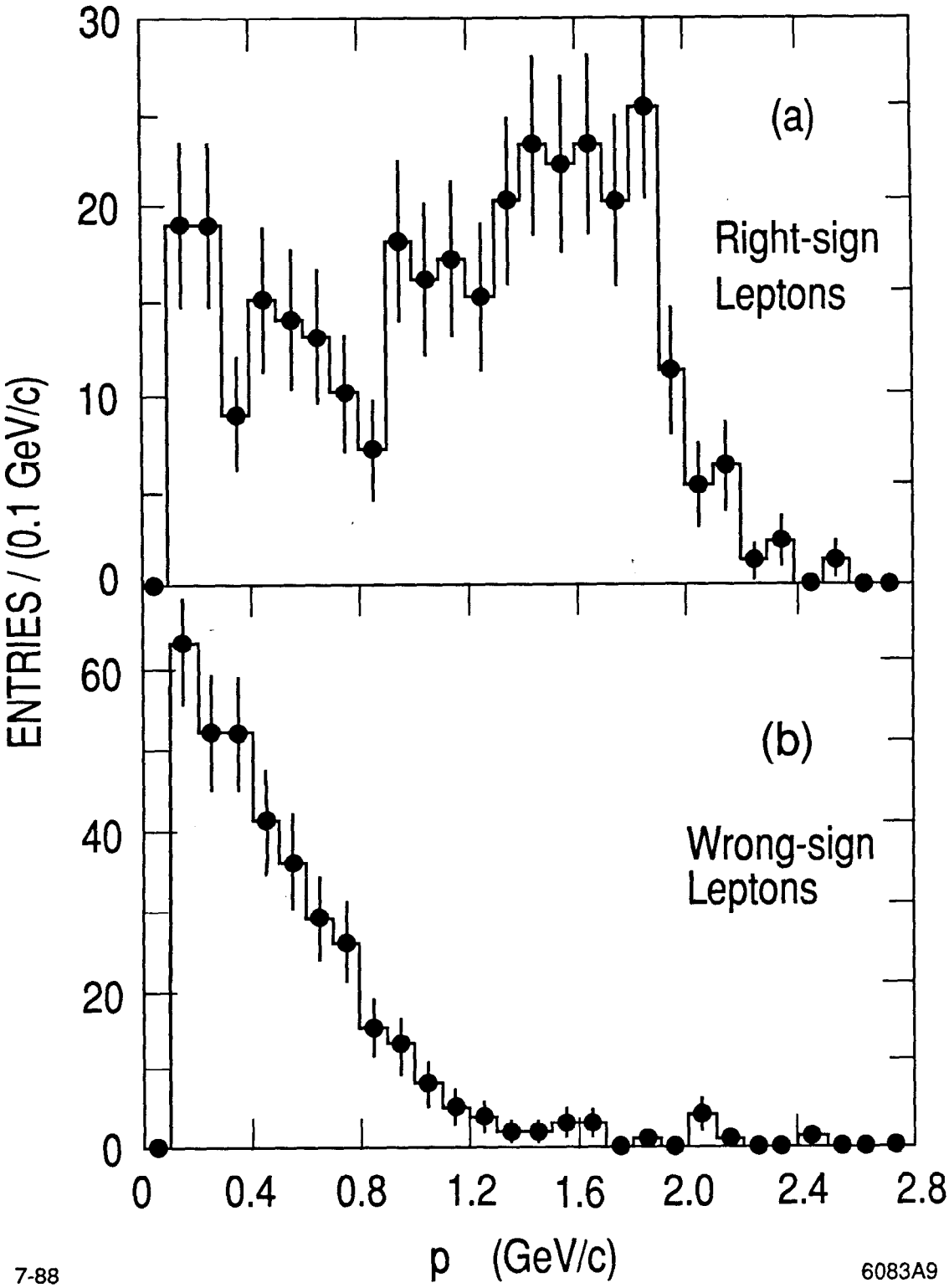
30
20
10
0
(a)
Right-sign
Leptons
ENTRIES / (0.1 GeV/c)
60
40
20
0
(b)
Wrong-sign
Leptons
0
0.4
0.8
1.2
1.6
2.0
2.4
2.8
p (GeV/c)
7-88
6083A9

Fig. 8

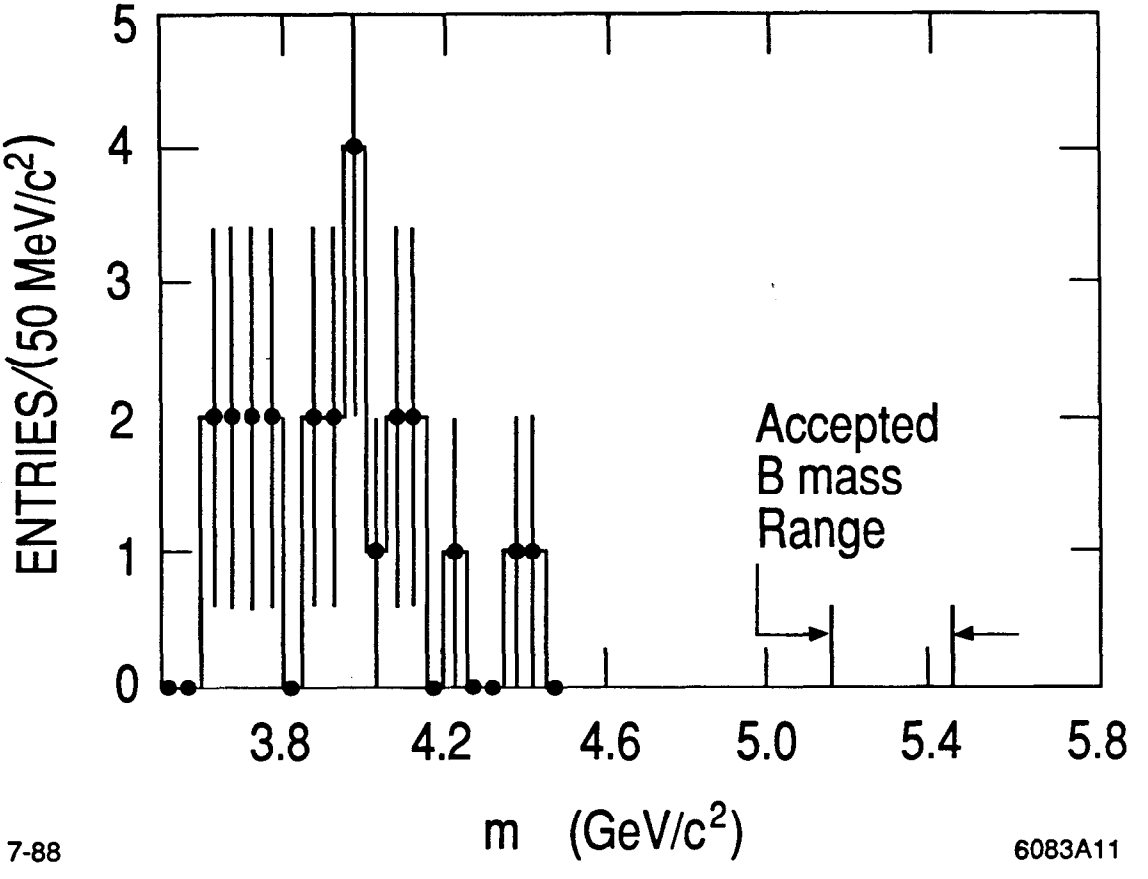
5
4
3
2
1
0
ENTRIES/(50 MeV/c²)
Accepted
B mass
Range
3.8
4.2
4.6
5.0
5.4
5.8
m (GeV/c²)
7-88
6083A11

Fig. 9

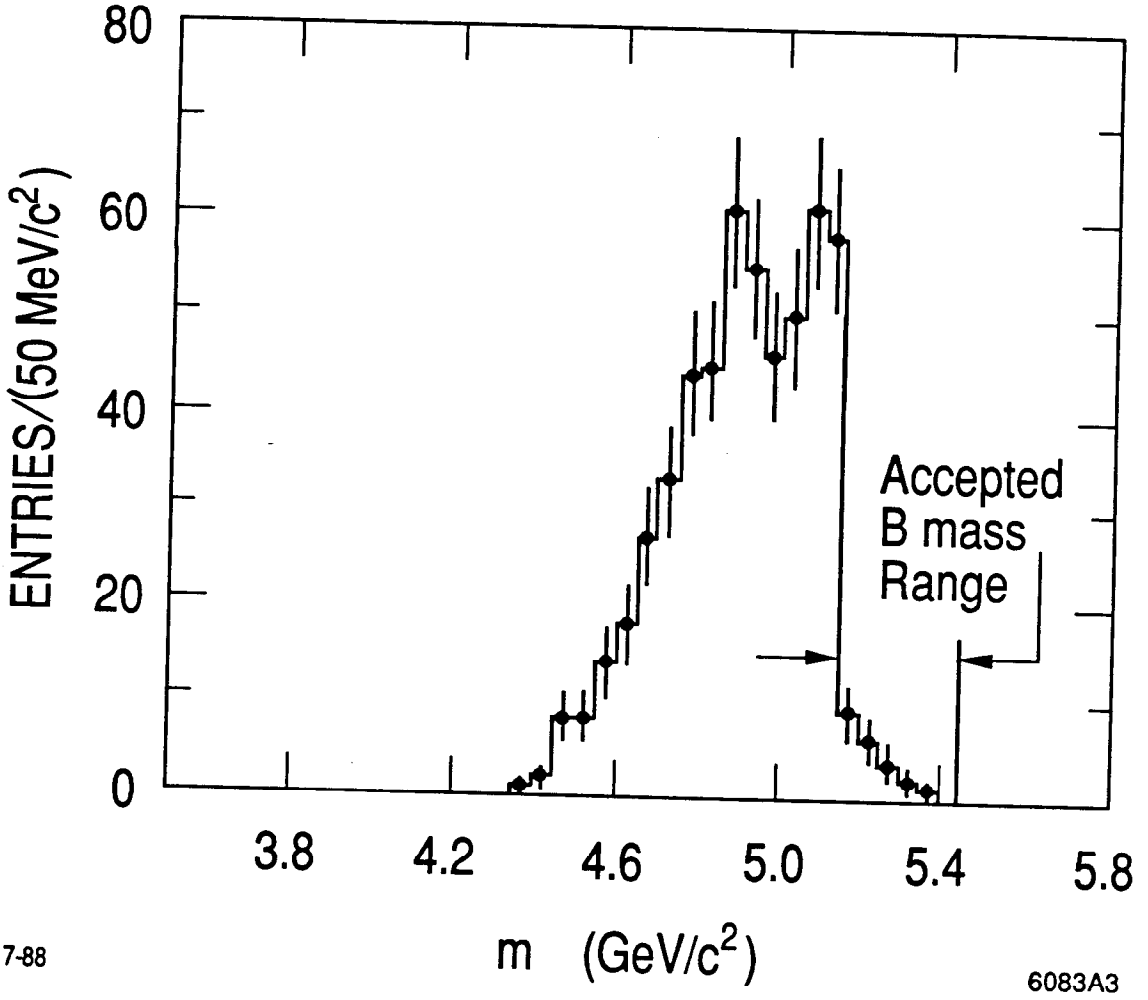
80
60
40
20
0
ENTRIES/(50 MeV/c²)
Accepted
B mass
Range
3.8
4.2
4.6
5.0
5.4
5.8
m (GeV/c²)
7-88
6083A3

Fig. 10

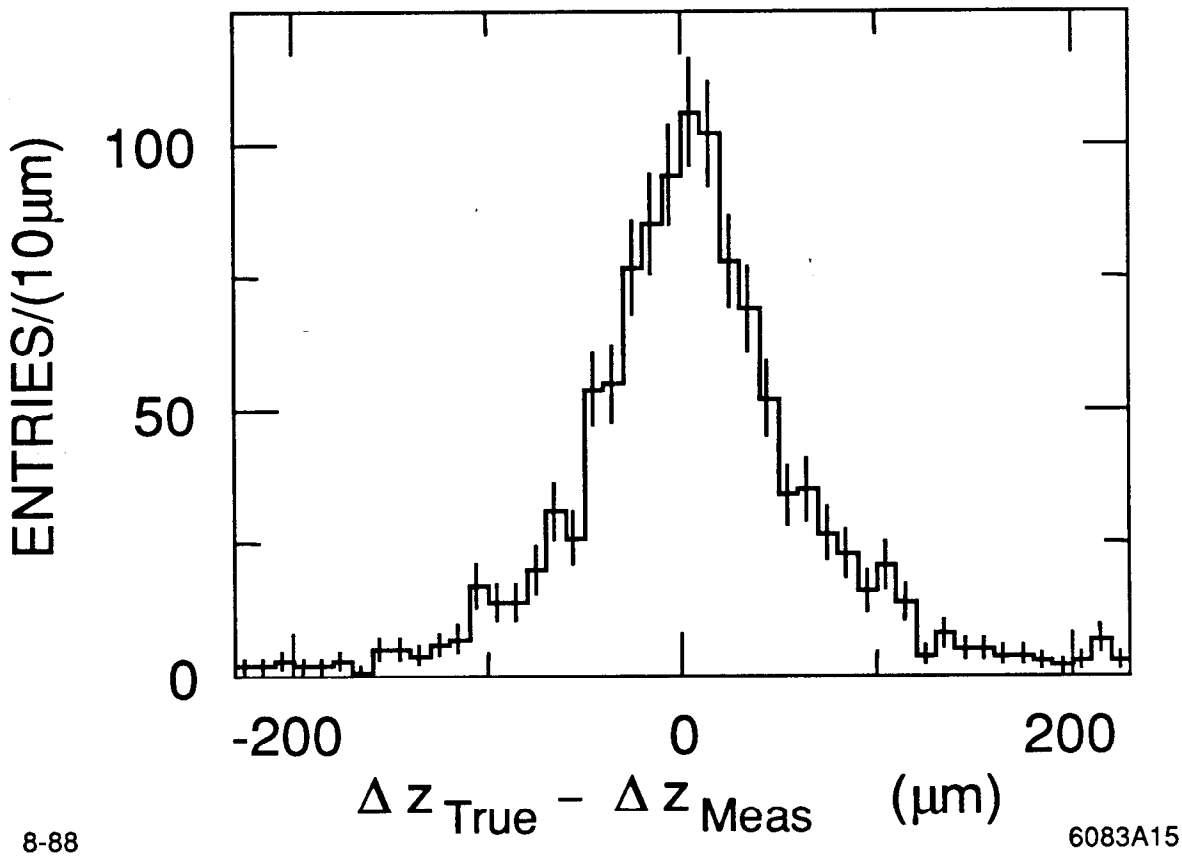

Fig. 11

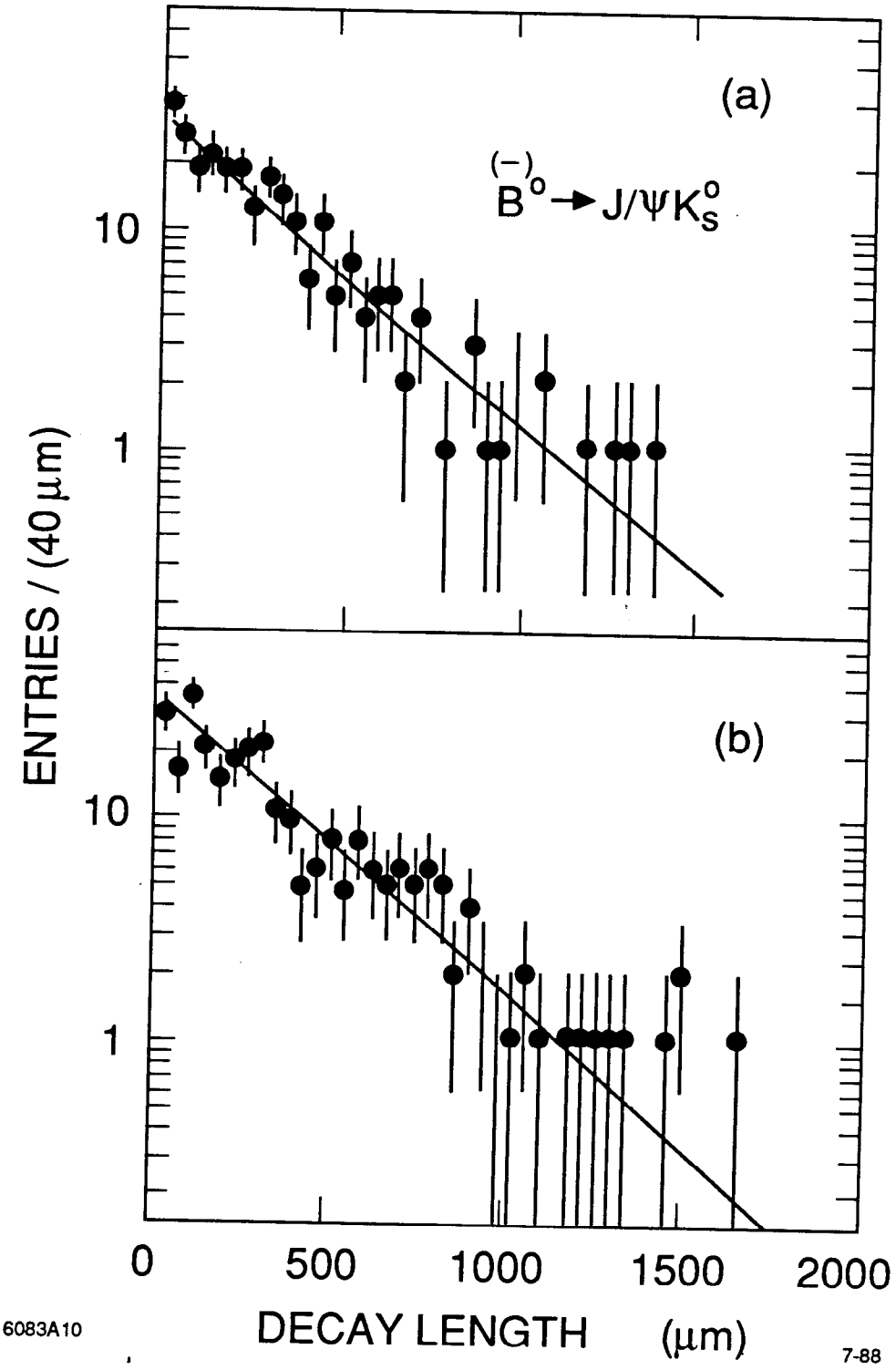
(a)
$\overset{(-)}{B}{}^{o} \rightarrow J/\psi K_s^o$
10
1
ENTRIES / (40 μm)
(b)
10
1
0
500
1000
1500
2000
DECAY LENGTH (μm)
6083A10
7-88

Fig. 12

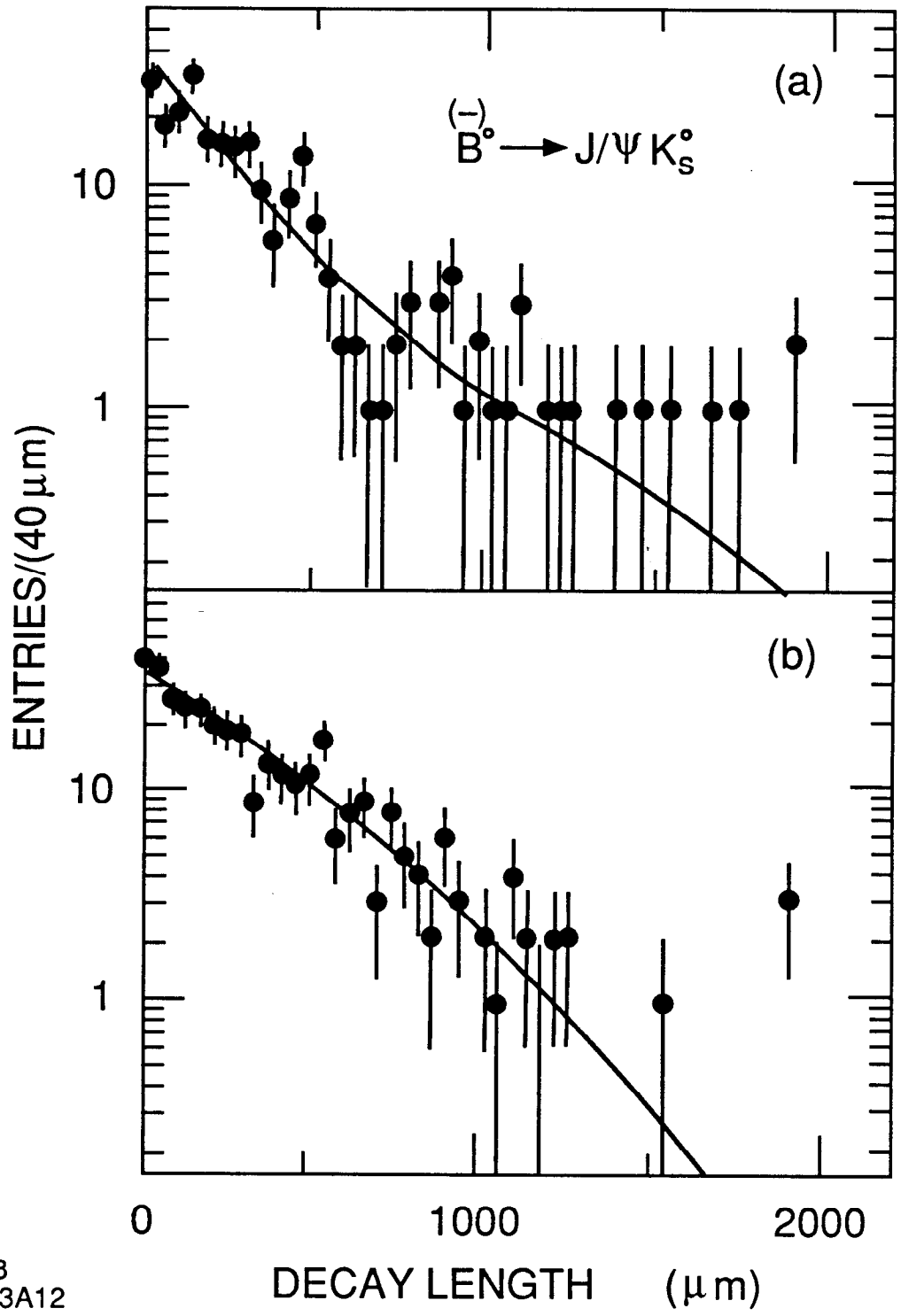
(a)
$\overline{B}^{\circ} \rightarrow J/\Psi K_S^{\circ}$
10
1
(b)
10
1
ENTRIES/(40 μm)
0
1000
2000
DECAY LENGTH (μm)
8-88
6083A12

Fig. 13

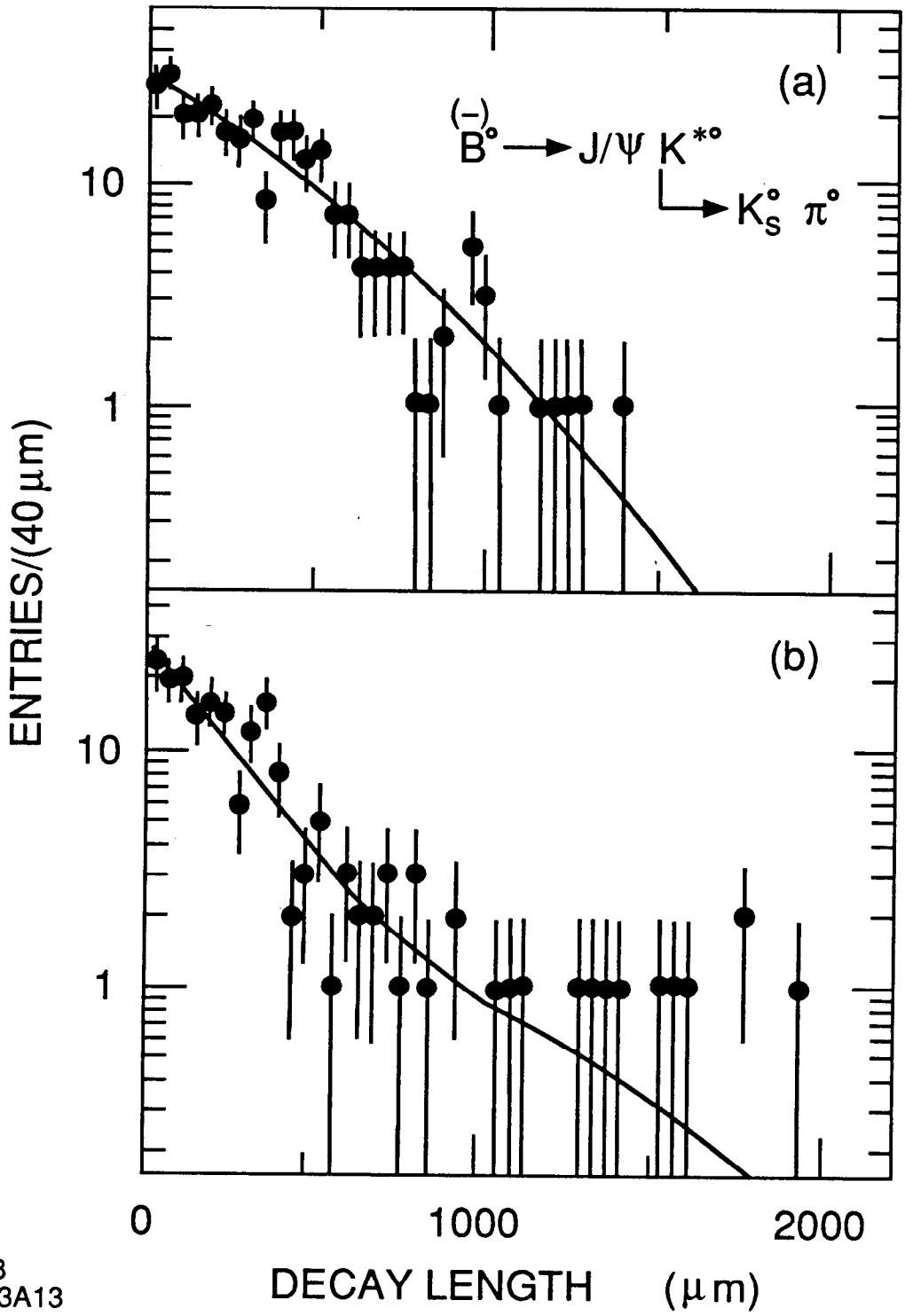
(a)
$\bar{B}^0 \rightarrow J/\psi\ K^{*0}$
$\hookrightarrow K_S^0\ \pi^0$
10
1
(b)
10
1
ENTRIES/(40 μm)
0
1000
2000
DECAY LENGTH (μm)
8-88
6083A13

Fig. 14